THE UNIVERSITY OF OKLAHOMA

GRADUATE COLLEGE

CRYSTAL AND MOLECULAR STRUCTURE ANALYSIS OF THE COPPER CHELATES OF L-SERINE AND GLYCYL-L-LEUCYL-L-TYROSINE

A DISSERTATION

SUBMITTED TO THE GRADUATE FACULTY

in partial fulfillment of the requirements for the

degree of

DOCTOR OF PHILOSOPHY

BY

WILLIAM A. FRANKS

Norman, Oklahoma

1968

CRYSTAL AND MOLECULAR STRUCTURE ANALYSIS OF THE COPPER CHELATES OF L-SERINE AND GLYCYL-L-LEUCYL-L-TYROSINE

APPROVED BY

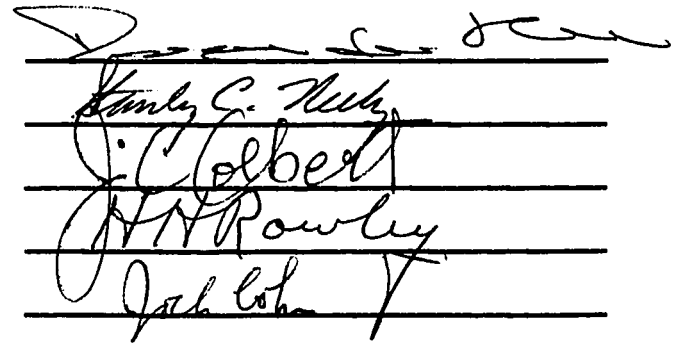

DISSERTATION COMMITTEE

ACKNOWLEDGEMENTS

The author wishes to express his appreciation to Dr. D. van der Helm for the suggestion of this research topic and for his patient direction throughout the course of the investigation.

The author gratefully acknowledges the support and assistance from N. I. H. grant GM-10514 obtained by Professor D. van der Helm. Programs used in this work are listed in Appendix II.

The author also wishes to acknowledge the aid of Mr. Charles Fisher who obtained crystals of the copper chelate of l-serine and determined the space group, and wishes to extend his thanks to his fellow graduate students who were around with a helping hand.

Also, the author wishes to thank Mrs. Evelyn Porterfield who typed this manuscript.

Lastly, the author is very grateful for the enduring patience and encouragement of his wife, Loretta and three children, Sharon, William II, and Leonard Earl and his parents, W. E. and Winnie.

TABLE OF CONTENTS

LIST OF TABLES

LIST OF FIGURES

CRYSTAL AND MOLECULAR STRUCTURE ANALYSIS OF THE COPPER CHELATES OF 1-SERINE AND GLYCYL-1-LEUCYL-1-TYROSINE

CHAPTER I

INTRODUCTION

The crystal and molecular structure analysis of the copper chelates of l-serine and glycyl-l-leucyl-l-tyrosine were initiated as part of an overall program for studying the interactions of transition metal ions with amino acids and peptides. The structures of small molecules such as amino acids and peptides are valuable in that these structures serve as models from which further knowledge of the structures of proteins, enzymes, and polypeptides can be obtained.

There were several interesting features of l-serine that made it suitable as a choice for a structure analysis. The copper chelate was readily crystallizable and the crystals were quite stable on exposure to the atmosphere. The l-serine itself contains three functional groups, amino, hydroxyl, and carboxyl which can donate ligand atoms for coordination to copper. Furthermore, the structure of dl-serine (1) is available for comparison

with the chelated molecule.

The tripeptide, glycyl-l-leucyl-l-tyrosine, was quite interesting in that it contained an isopropyl and a phenolic group attached to two of the three alpha carbon atoms. Crystals of this complex were not readily obtainable and the crystal decomposed on exposure to the atmosphere. Another disheartening feature of the chelate was that it contained two peptide molecules and two copper ions in the asymmetric unit.

A study of this nature is encouraged by the fact that one can obtain direct evidence regarding the coordination configuration surrounding the copper ions, and any changes in bond angles and distances that occur as a result of chelation. The results of previous studies on the copper chelates of amino acids and peptides have been summarized (2). The α-amino acids included in this summary were (I) bis glycinato copper (II) hydrate (3,4), (II) bis (dl-α-aminobutyrato) copper (II) (5), (III) bis (1-amino cyclopentanecarboxylato) copper (II) (6), (IV) bisprolinato copper (II) dihydrate (7), and (V) glutamato copper (II) dihydrate (8). The copper ion was 6 surrounded in (I), (III), (IV), and (V). The structure of compound (II) was incomplete. The copper ion was located on a center of symmetry in (II), (III), and (IV) which required the four closest ligand atoms to be in the same plane with the copper ion and coordinated trans with

respect to each other. When the copper ion was not located on a center of symmetry, it deviated from the best least squares plane of the four closest ligand atoms in the direction of the closest apex atom. The cis configuration was observed for compound (I) and it was reported that this is the only known example of the cis configuration. The coordination of copper ions and l-serine ions have been studied in solution. Li and Doody (9) postulated that when copper (II) ions and l-serine ions were brought together in a 1:2 mole ratio respectively that a 1:2 complex was present in solution with an absorption maximum in the region of 615 to 650 millimicrons. The structure so proposed was a dimer with the trans configuration. Spectral evidence obtained on a 1:1 mole ratio of the complex show an absorption near 700 millimicrons. The difference between the complex formed from a 1:2 mole ratio and the complex formed from a 1:1 ratio was also evident in their colors. The 1:2 complex was blue whereas the 1:1 complex was bluish violet. The crystal and molecular structure of the copper chelate should lead to the correct configuration around the copper ion and yield further knowledge on the coordination chemistry of amino acids.

The coordination of copper ions and tripeptide ions have been investigated in the complexes of (VI) glycylglycylglycylinato copper (II) chloride sesquihydrate (10) and (VII) sodium glycylglycylglycylinato copper (II)

hydrate (11). Also, the structure of a tetrapeptide complex, (VIII) disodium glycylglycylglycylglycinato copper (II) decahydrate (12), is known. The copper ion was 6 surrounded in (VI), 5 surrounded in (VII), and 4 surrounded in (VIII). The interesting feature of the latter complex was that four nitrogen atoms of one peptide molecule served as the ligand atoms.

The configuration of proteins and polypeptides was proposed by Pauling and Corey (13). The following conditions for a polypeptide structure were established by them:

1. The peptide system is always planar because of resonance

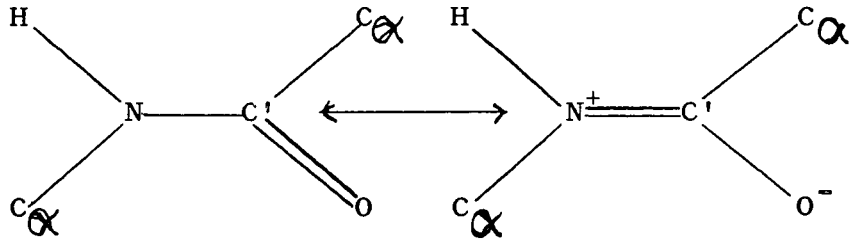

2. The bond lengths are those given below.

C_α——C'	C'——O	C'——N	N——C_α
1.53 A°	1.23 A°	1.32 A°	1.47 A°

3. Every C'——O group and every N-H group is involved in hydrogen bonding.
4. The C'——O and N-H bond have the trans configuration.

Two different structures were postulated depending on the orientation of the peptide units. The two structures so proposed were the helical and pleated sheet. These

two structures are generally observed in proteins and polypeptides. Also, the parallel-chain pleated sheet configuration has been observed in the tripeptide glycyl-l-phenylalanyl-glycine (14). Recently Ramakrishman and Ramachandran (15) have published conformational maps showing the allowed orientations of peptide units within the peptide and polypeptide molecules. Only certain orientations are allowed due to restrictions established by intramolecular contact distances. The structure of the copper chelate of glycyl-l-leucyl-l-tyrosine will give further evidence concerning the configuration of peptides and their coordination with copper ions.

CHAPTER II

CRYSTAL AND MOLECULAR STRUCTURE OF THE COPPER CHELATE OF l-SERINE

Experimental Measurements

The complex bis (l-serinato) Cu(II) was prepared by reacting two moles of l-serine with one mole each of barium hydroxide and copper sulfate giving a solution 0.1 molar in l-serine. Barium sulfate was removed from the solution by filtration. Crystals of this complex were obtained by diluting the chelate solution to 100 times its volume with absolute ethanol. Small blue crystalline rectangular plates appeared on standing two or three days at room temperature. The density was determined as 1.90 by the flotation method. The crystals were monoclinic, space group $P2_1$ with two molecules in the unit cell. The cell dimensions were determined by the method of least-squares using twenty-six general reflections. Using the cell dimensions and observed density, a molecular weight of 271 was calculated for the asymmetric unit. The complex contained one mole of copper and two moles of l-serine with a molecular formula of

$$Cu(C_3 H_6 O_3 N)_2.$$

The crystal data are shown in Table 1.

The mosaic properties of the crystal were determined using a method described by Furnas (16). The intensities of the 100, 040, and 002 hkl reflections were measured as a function of the omega angle. These results were then graphed and are shown in Figure 1. The size of the crystal used in the experiment was 0.02", and the intensities were measured at a 1^{o} take-off angle. The mosaic of the crystal was calculated by taking the difference between the width of the base of the curve and the width of the crystal. A mosaic spread of 1.0^{o} was obtained for the 100 reflection and 0.9^{o} for both the 040 and 002 reflections. The mosaic of the crystal is larger than one would normally expect. The mosaic spread of most crystals is less than 0.5^{o}. The graphs for the 100 and 002 reflections in Figures 1a and 1b show the intensity peaks separate into two unresolved peaks, and the separation is largest for the 100 reflection. The unresolved peaks and large mosaic of the crystal suggest that the crystals should be investigated for twinning. Measurements were carried out to assess qualitatively any twinning within the crystals. Intensities of several h0l and $h0\bar{l}$ reflections were measured on four different crystals. The ratio, $h0\bar{l}$:h0l, for each pair of reflections was computed and the results are listed in Table 2.

Twinning within the crystals was qualitatively

TABLE 1

Crystal Data of bis (l-Serinato) Cu(II)

Space Group	$P2_1$
No. of Molecules	2
Cell Dimensions	
a =	$9.924 \pm .003$
b =	$8.413 \pm .002$
c =	$5.615 \pm .001$
β =	$90.64 \pm .02$
Density	
Obs.	= 1.90
Calc.	= 1.91
Vol.	471.76
F(000)	274

TABLE 2

Ratio between $I(h0\bar{1})$ and I(h01) for Four Crystals

h01	A	B	C	D	Ave.
$20\bar{1}$:201	.3288(+)	.2752(-)	.3015(-)	.3058(+)	.3037
$40\bar{2}$:402	.0395(-)	.0405(+)	.0410(+)	.0407(+)	.0401
$60\bar{3}$:603	.2714(+)	.2846(+)	.2654(+)	.2596(-)	.2702
$80\bar{4}$:804	1.2524(-)	1.3897(+)	1.3186(+)	1.2252(-)	1.2964
$30\bar{1}$:301	11.5433(+)	11.3607(+)	11.4758(+)	10.9724(-)	11.3380
$60\bar{2}$:602	.6044(+)	.6203(+)	.6023(+)	.5716(-)	.5996
$90\bar{3}$:903	1.0939(-)	1.2408(+)	1.1291(+)	1.1182(-)	1.1455
$40\bar{1}$:401	1.3651(-)	1.3389(-)	1.3970(+)	1.3683(+)	1.3673
$80\bar{2}$:802	.7173(-)	.7993(+)	.7449(-)	.7221(-)	.7459

Figure 1. Intensity versus Omega Angle for (A) 100, (B) 002, and (C) 040 Reflections.

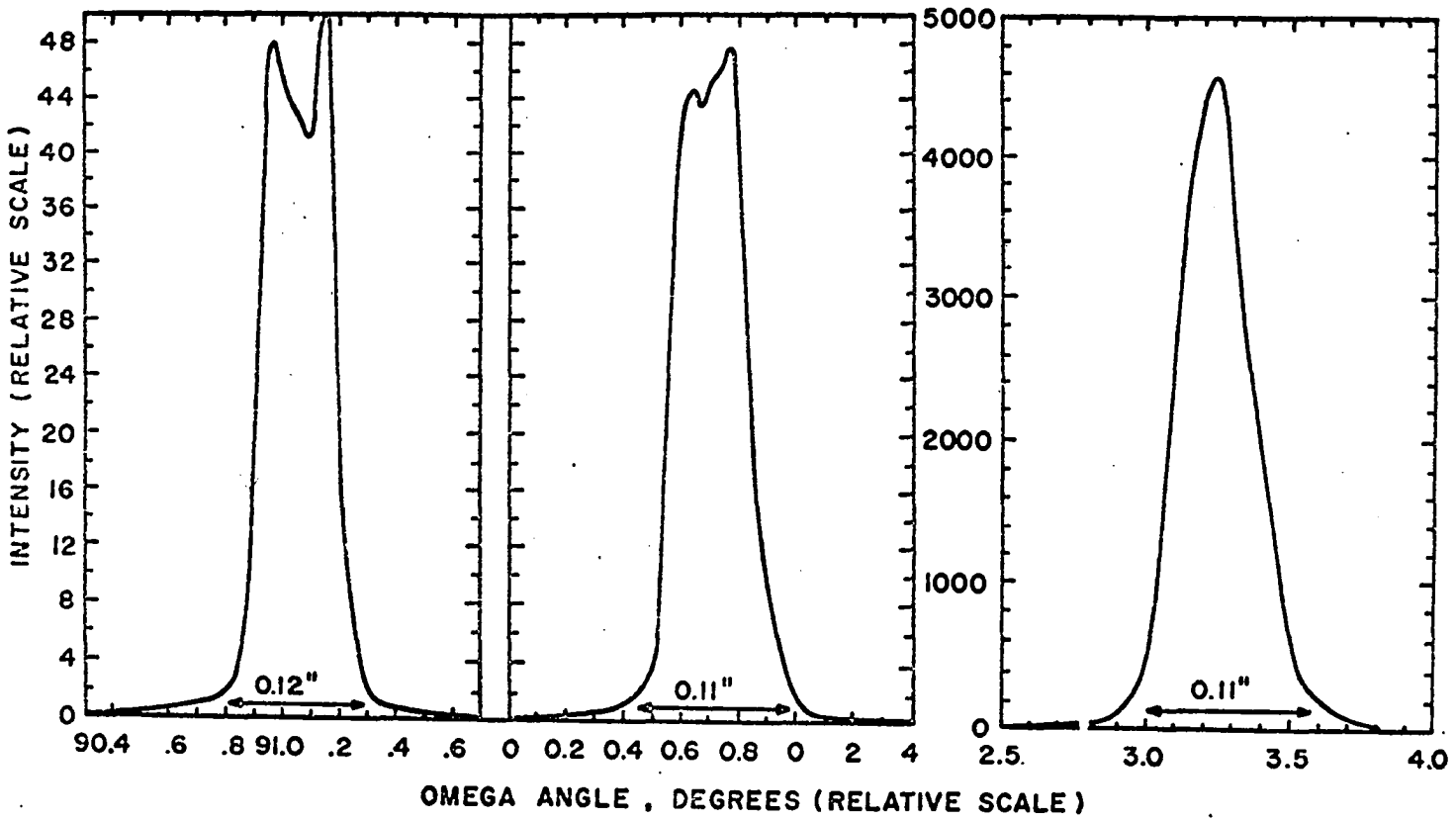

assessed by observing the deviation of the ratio of each pair of $h0\bar{l}$ and h0l reflections from the mean or average ratio. These deviations are shown as either (+) or (-) in Table 2. Crystals B and C had a larger number of positive deviations than negative deviations, and crystal D had a larger number of negative deviations than positive deviations. This data indicate qualitatively that a small amount of twinning exists in the crystals. However, the assumptions were made that the amount of twinning and crystal imperfections would not interfere with the structure determination.

The crystal chosen for intensity measurements was cut from a large plate and mounted with b* parallel to the polar axis. Intensities were collected using a theta-two theta scan with a 1^{o} take-off angle. Monitor values were taken every 100 to 125 reflections, and only one crystal was used to collect 934 observed and 12 unobserved amplitudes out to a two theta value of 140^{o}. Absorption and Lorentz-Polarization corrections were applied to the data.

Determination and Refinement of Trial Structure

A sharpened Patterson synthesis was calculated to obtain the location of the copper atom. The map was sharpened by multiplying $|F|^2$ by the function (17)

$$M(S) = \left\{ \frac{\sum Z_i}{\sum f_i} \right\}^2 \exp(-2.10 \sin^2 \Theta / \lambda^2)$$

$\sum Z_i$ = Sum of the atomic numbers

$\sum f_i$ = Sum of the scattering factors at $\sin \theta / \lambda$ of the amplitude which is modified.

One-fourth of the unit cell was calculated on a grid (UVW) with grid points approximately $0.2A^{o}$ apart. Sections were computed perpendicular to the b axis. The equivalent positions of space group $P2_1$ are

$$X, Y, Z$$

$$\overline{X}, \tfrac{1}{2} + Y, \overline{Z} .$$

Defining the vector between the copper atoms as HH, the vectors between light atoms as LL, and the vectors between copper and light atoms as HL, their respective vector equations and relative peak heights are given as

$$\frac{U}{2X} \qquad \frac{V}{\frac{1}{2}} \qquad \frac{W}{2Z}$$

HH = 841 LL = 64(max.)

X_2-X_1 Y_2-Y_1 Z_2-Z_1

HL = 234(max.) L_1L_2 = 64(max.)

X_2+X_1 $\frac{1}{2}+Y_2-Y_1$ Z_2+Z_1

HL = 234(max.) L_1L_2 = 64(max.)

Relative peak heights were calculated with the relation

$$(Z_1 \times Z_2)$$

where Z_1 and Z_2 are the atomic numbers of atoms one and two respectively. The relative peak heights are only qualitative since sharpening will change the relative heights as will the thermal motion of the atoms. The largest peak (600) in the Harker section V=½ was assumed to be the HH vector from which the coordinates of the copper atom were calculated. In space group $P2_1$, the origin of the unit cell can be located anywhere along the b axis. The Y-coordinate of copper was chosen as ½. The Patterson map was so well resolved that a search for other atoms seemed feasible. Utilizing the assumption that the peaks above 200 in the map were due to HL vectors, a search for these vectors was initiated. Each pair of HL vectors was found for all the light atoms. Furthermore, no peaks above 200 remained after this search which indicated we were on the right course. Due to the false mirror plane introduced by the Patterson function, the Y-parameter of any light atom could either be +Y or -Y. This ambiguity was removed by constructing a model of the complex and assigning to it the absolute configuration of l-amino acids. The exception to this was one hydroxyl oxygen which was quite close to the mirror plane and we were not able to determine if the parameter should be +Y or -Y. This atom was initially assigned the +Y parameter. Structure Factors were

calculated for this trial structure giving a reliability index $\left(= \frac{\sum|\Delta F|}{\sum|kF_o|} \right)$ of 0.195.

The trial structure was refined by three-dimentional block diagonal least squares. The following weighting scheme was used in least squares calculations;

$$\sqrt{W} = |F_o|/P_1 \text{ if } |F_o| \leq P_1,$$

or

$$= P_1/|F_o| \text{ if } |F_o| > P_1.$$

The value of P_1 was taken as 17.0. Initial refinement was carried out isotropically with subsequent anisotropic refinement of the atoms in later cycles. Of particular note in the early stages of isotropic refinement was the continued large positive ΔB along with a continued negative shift in the Y-parameter of the one hydroxyl oxygen which was assigned the +Y value from the Patterson map. Consequently the Y-parameter of this atom was changed from the original +Y value to -Y where upon negative isotropic shifts were obtained. We should state that the hydroxyl oxygens could have been correctly located from a Fourier synthesis. Hydrogen atoms were initially located from a difference Fourier synthesis with the aid of atomic positions calculated from an assumed tetrahedral surrounding of the central atom. The model from which the approximate positions of the hydrogens were obtained is shown in

Figure 2.

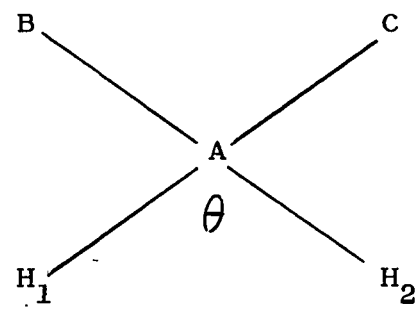

Figure 2.--Tetrahedral Model

A is the central tetrahedrally surrounded atom, B and C represent atoms bonded to A with known atomic positions, and H_1 and H_2 are the parameters in question. To calculate the position of H_1 we have the following two vector equations.

$$\text{Cos}\,\theta = \overline{AC} \cdot \overline{AH}_1 \quad (1)$$

$$\text{Cos}\,\theta = \overline{AB} \cdot \overline{AH}_1 \quad (2)$$

Where θ is the tetrahedral angle of $109^{\circ}20'$. The third equation originates from the fact that the vector $\overline{AH}_1$ makes an angle of $54^{\circ}45'$ with the plane defined by the atoms A, B, and C. Letting $\overline{n}$ represent the normal to this plane, then

$$\text{Cos}\ 54^{\circ}45' = \overline{AH}_1 \cdot \overline{n} \quad (3)$$

These three equations are then simultaneously solved for the parameters XYZ. The parameters of H2 can be calculated from the relations

$$\text{Cos}\,\theta = \overline{AC} \cdot \overline{AH}_2$$

$$\text{Cos}\,\theta = \overline{AB} \cdot \overline{AH}_2$$

$$\text{Cos}\,\theta = \overline{AH}_1 \cdot \overline{AH}_2$$

This procedure was carried out for all atoms with hydrogens bonded to them with the exception of the hydroxyl oxygens which were not tetrahedrally bonded. The difference Fourier map was calculated at an R-Index of 0.0600, and the hydrogen atoms were located at peaks having the estimated height for a hydrogen atom and occurring close to their calculated positions. The hydroxyl hydrogens were located approximately $1A^{o}$ from the oxygen along the vector between the oxygen and the hydrogen bonded acceptor atom. The hydrogen atoms were included in the structure factor calculations but not refined.

Anamolous dispersion corrections were applied to the crystal. The atomic scattering factor can be written as

$$f = f_0 + \Delta f' + i\,\Delta f''$$

where f_0 is the scattering of the 'free' electrons, and $\Delta f'$ and $\Delta f''$ are the real and imaginary dispersion corrections arising from bound electrons. Dispersion effects arise mainly from the innermost electrons when the frequency of the incident radiation is nearly equal to the frequency of the electronic transitions for these electrons. The dispersive effects due to the light atoms were either

zero or very small and need not be corrected. However, $\Delta f'$ and $\Delta f''$ for the copper atoms were -2.1 and -0.7 respectively with $CuK\alpha$ radiation and dispersions corrections were made for these atoms using most of a procedure developed by Patterson (18).

Anamolous dispersion corrections were applied directly to $_{+}F_{o}(hkl)$ and not to the geometrical mean of $_{-}F_{o}$ and $_{+}F_{o}$ as suggested by Patterson.

The structure was further refined until the shifts were less than one-third the estimated standard deviations. At this point another difference map was calculated and the hydrogens atoms relocated. This difference map did not show the presence of one of the hydroxyl hydrogens. The new positions of the hydrogen atoms found from the difference map were included in more least-squares cycles but not refined. The refinement was completed when the shifts for all parameters again became lower than one-third the estimated standard deviations. The final parameters and their estimated standard deviations are shown in Table 3. The observed and calculated amplitudes along with the phase angles are listed in Table 1 of Appendix I.

Discussion of the Structure

Accuracy of the Results.

The agreement between the observed and calculated Structure Factors is one means of assessing the accuracy of a structure determination. The final Structure Factor

TABLE 3

Atomic Parameters of bis(l-Serinato) Cu(II)

Atom	X	Y	Z
Cu	0.3182(.0001)	0.4999(.0002)	0.4861(.0001)
O_1A	0.4667(.0005)	0.3448(.0007)	0.5018(.0010)
O_2A	0.6169(.0005)	0.2188(.0006)	0.2780(.0009)
C_1A	0.5356(.0006)	0.3282(.0008)	0.3147(.001)
C_2A	0.5103(.0007)	0.4503(.0008)	0.1150(.0010)
C_3A	0.6419(.0006)	0.5125(.0010)	0.0223(.0010)
O_3A	0.7180(.0005)	0.5791(.0007)	0.2098(.0010)
N(A)	0.4202(.0006)	0.5785(.0007)	0.2088(.0010)
O_1B	0.2403(.0005)	0.3960(.0006)	0.7615(.0009)
O_2B	0.0747(.0006)	0.4153(.0008)	1.0186(.0010)
C_1B	0.1313(.0007)	0.4585(.0008)	0.8367(.0010)
C_2B	0.0714(.0007)	0.5956(.0009)	0.6901(.0010)
C_3B	-0.0793(.0008)	0.5895(.0010)	0.6737(.0010)
O_3B	-0.1191(.0005)	0.4496(.0006)	0.5537(.0010)
N(B)	0.1388(.0006)	0.6002(.0007)	0.4571(.0010)
$H(C_2A)$	0.470	0.390	-0.020
$H_1(C_3A)$	0.670	0.400	-0.080
$H_2(C_3A)$	0.650	0.610	-0.090
$H_1(NA)$	0.375	0.620	0.110
$H_2(NA)$	0.490	0.640	0.260
$H(C_2B)$	0.110	0.700	0.800
$H_1(C_3B)$	-0.110	0.610	0.810
$H_2(C_3B)$	-0.110	0.690	0.580
$H(O_3B)$	-0.170	0.500	0.460
$H_1(NB)$	0.120	0.500	0.340
$H_2(NB)$	0.130	0.680	0.400

TABLE 3a

Anisotropic Temperature Values

				$\times 10^4$		
Atom	b11	b22	b33	b23	b13	b12
Cu	38(1)	46(1)	133(2)	39(5)	32(2)	18(3)
O_3B	70(10)	63(10)	256(20)	21(20)	-91(20)	12(10)
O_2B	95(10)	107(10)	161(20)	72(20)	105(20)	22(10)
O_1B	57(10)	62(10)	156(20)	60(20)	38(10)	27(10)
O_1A	63(10)	79(10)	151(20)	71(20)	73(20)	73(10)
O_2A	62(10)	53(10)	147(20)	89(20)	19(10)	33(10)
O_3A	57(10)	78(10)	250(20)	-51(20)	-49(20)	-53(10)
N(B)	49(10)	37(10)	119(20)	22(20)	29(20)	22(10)
N(A)	47(10)	35(10)	120(20)	10(20)	-10(20)	22(10)
C_3B	63(10)	61(10)	172(20)	-48(30)	37(20)	-19(20)
C_2B	44(10)	70(10)	106(20)	-25(20)	50(20)	41(10)
C_1B	44(10)	73(10)	176(20)	-23(20)	66(20)	-39(10)
C_3A	53(10)	52(10)	177(20)	17(30)	45(20)	-15(20)
C_2A	42(10)	52(10)	103(20)	11(20)	13(20)	39(11)
C_1A	28(10)	45(10)	178(20)	47(20)	-11(20)	22(10)

calculation with all reflection gave an R-index of 0.040. Standard deviations were calculated for each atomic parameter, and these are shown in Table 3. The average value of the estimated standard deviations for the light atoms are 0.006A, 0.007A, and 0.006A for the coordinates x, y, and z. Further assessment of the accuracy is obtainable from the difference Fourier and composite Fourier (Figure 3). Two negative peaks of heights -1.1 and -1.0 $e/A^{o\ 3}$ occur along with two positive peaks of heights 1.2 and 1.0 $e/A^{o\ 3}$ around the atomic position of copper in the difference Fourier (not shown). This effect is attibuted to inaccuracies of the anisotropic temperature factors for copper. However, most of the experimental errors that are inherent in a structure determination are minimized by adjustment of the anisotropy of an atom. Therefore, anisotropic temperature factors compensate not only for the thermal motion of an atom but also for those errors whose corrections were not applied to this structure. Similar effects for the light atoms were not observable in the difference Fourier. The observed electron density calculated with the observed amplitudes are shown in Table 4.

Structure of bis (l-Serinato) Cu(II)

Figure 4 shows the complex projected onto the ac plane. The complex is a dimer formed from the coordination of two l-serine molecules to copper via the amino nitrogens and a carboxylic oxygen from each serine molecule. The two

Figure 3. Composite Fourier of bis(l-Serinato) Cu(II)

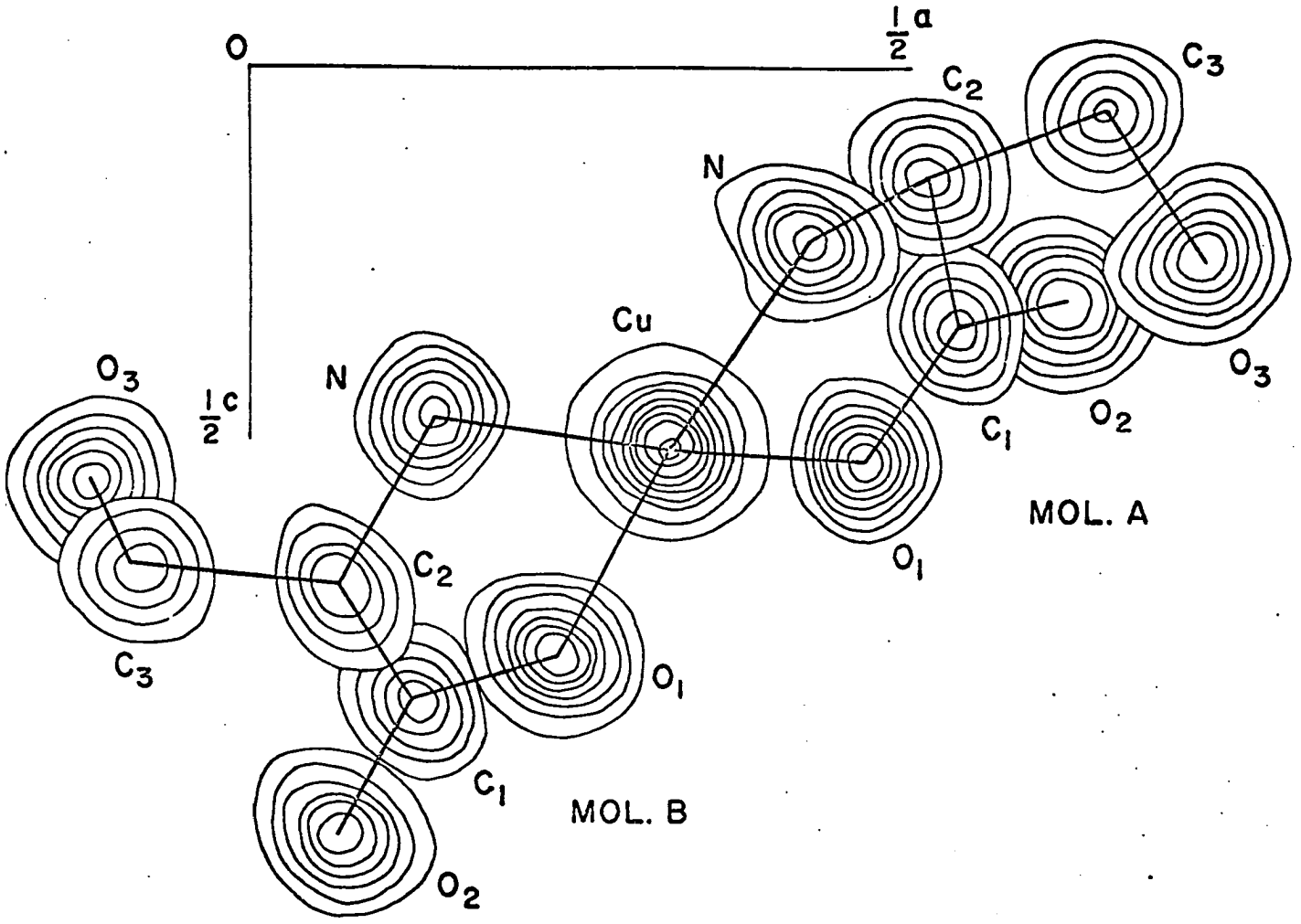

TABLE 4

Electron Density of the Atoms, e/A^{o}(3)

Atom	Molecule A	Molecule B
C_1	10.6	10.3
C_2	10.2	9.9
C_3	10.1	9.4
O_1	14.7	15.4
O_2	13.9	13.5
O_3	13.4	12.5
N	13.0	13.4
$H(C_2)$	0.5	0.5
$H_1(C_3)$	0.5	0.3
$H_2(C_3)$	0.5	0.4
$H_1(N)$	0.5	0.7
$H(O_3)$	-	0.7
$H_2(N)$	0.4	0.3
Cu	82.0	

Figure 4. ac Projection of bis (l-Serinato) Cu(II).

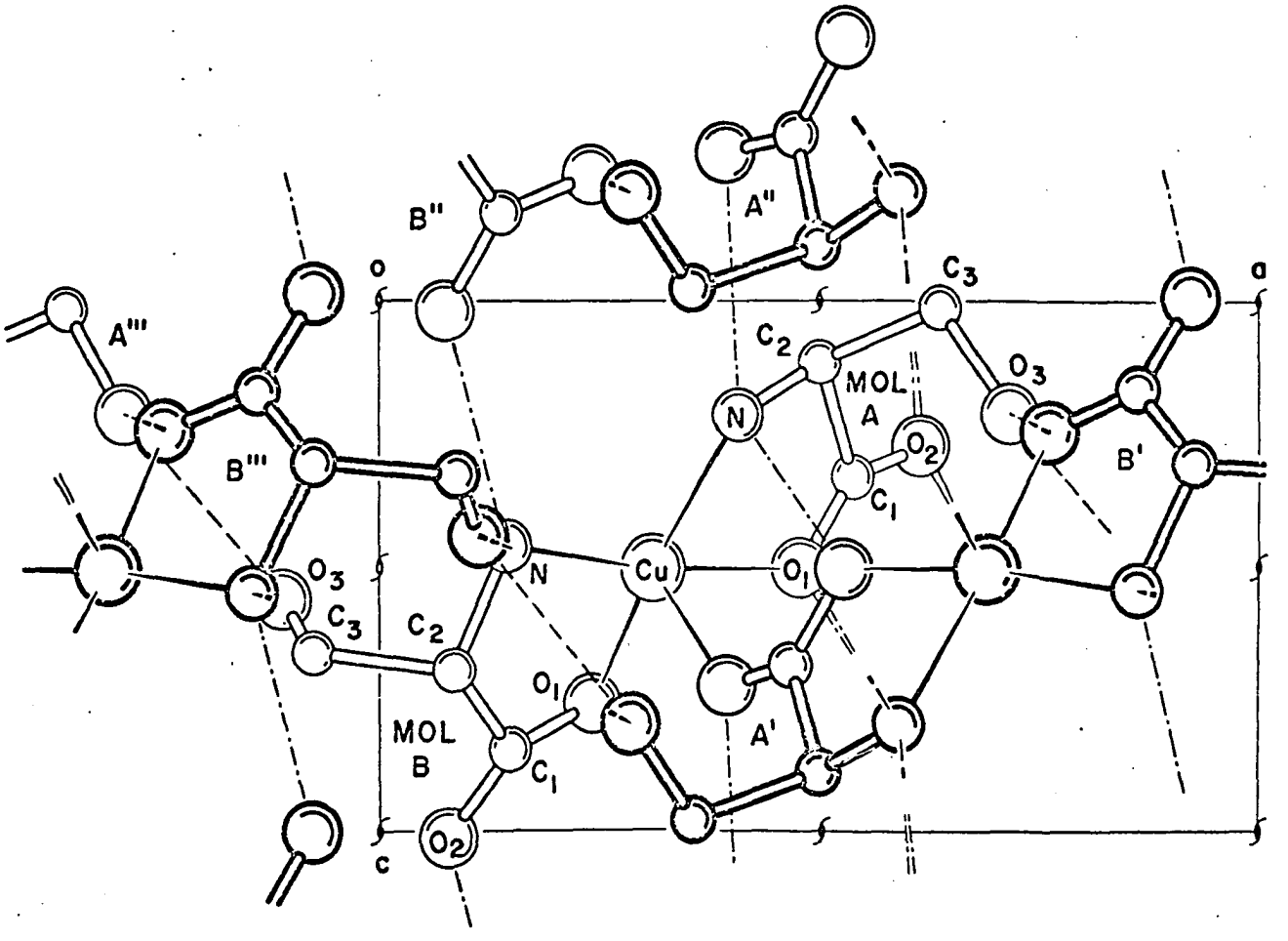

l-serine molecules are coordinated cis with respect to each other. One serine molecule is further coordinated to copper via the carboxylic oxygen of a symmetry related molecule. The copper atom is five surrounded and one l-serine molecule is shared by two copper atoms. The l-serine molecule that is shared by two copper atoms is referred to as the A molecule and the one not shared is referred to as the B molecule in Figure 4. The atoms comprising the asymmetric unit are labeled in Figure 4 without asterisks.

The molecule is nearly planar, and the best least squares plane for all atoms except C_3, O_3 and hydrogen atoms is nearly coincident with the 653hkl plane. The molecules extend more or less along the diagonal of the ac projection. The hydrogen bond between O_3B and O_3A''' packs molecules related by a translation along the a axis. This hydrogen bond is the only strong link between molecules related by a translation along the a axis. A van der Waals' interaction occurs in this direction between O_3A''' and C_3B of length 3.29A°. One hydrogen bond occurs between molecules related by a translation along the c axis. The hydrogen bond is between N(B) and O_2B'' of length 2.99A°. Van der Waals' interactions occurring in this direction are between N(A) and O_1B'' of length 3.44A° and C_2A and O_1B'' of length 3.36A°. The packing of the molecules in the a and c directions is a consequence of two hydrogen bonds and three van der Waals' interactions.

The packing in the third dimension or along the b axis is determined by the molecules related by a 2-fold screw axis. As was described earlier the molecules in the asymmetric unit are nearly coincident with the 653hkl plane. The molecules related by a 2-fold screw operation are then close to the $\bar{6}5\bar{3}$hkl plane. These two planes containing symmetry related molecules are "skewed" with respect to each other and separated by ½b. In Figure 4 the direction of the two planes can be observed. The symmetry related molecules fill the gap between molecules related by a translation along the c axis. The coordination between copper ions and carboxylic oxygens O_2A form the strong link between molecules related by the two-fold screw axis. Packing in this direction is further aided by four hydrogen bonds. The first is between O_3A and O_1B' of length 2.70A°, the second between N(A) and O_1A' of length 2.99A°, the third between N(B) and O_3B''' of length 2.95A°, and the fourth between N(A) and O_2A'' of length 3.01A°. Six van der Waals' interactions occur between symmetry related molecules: (1) N(A)----C_1A', 3.44A°; (2) C_2B----O_3B''', 3.32A°; (3) C_2B----O_2A', 3.27A°; (4) C_1B----O_2A', 3.39A°; (5) O_3A----O_1A', 3.33A°; (6) C_2A----O_2A'', 3.40A°. The open space in the 6th position around the copper ion forms an unoccupied column parallel to the b axis throughout one unit cell. The vacancy at the 6th position of the copper ion is partially filled by O_2B'' which

comes within a distance of 3.63A° to the metal and is further terminated to an extent by the van der Waals' interaction of C_3A'' and C_3B''' of length 3.48A°. In summarizing, the molecules are packed together as a series of parallel-skewed planes of molecules. The packing of the molecules is done primarily by the coordination of copper to a symmetry related carboxylic oxygen and six hydrogen bonds formed from all available protons. Ten van der Waals' interactions of less than 3.50A° aided in the packing of the molecules; however, five of the ten van der Waals' interactions were between atoms whose immediate neighbors were involved in hydrogen bonding to the same atoms. Hydrogen bond distances and angles are summarized in Table 5 along with the van der Waals' interactions of less than 3.50A°.

The configuration of l-serine molecules A and B are shown in Figure 5 along with one calculated for dl-serine (1). The dihedral angle between the plane of N, C_2, and C_3 and the plane of O_3, C_3, and C_2 are 66°22' for molecule A and 61°53' for molecule B. The hydroxyl group is rotated from the amino nitrogen towards the carboxyl group for both molecules A and B. In molecule A the hydroxyl oxygen is 2.96A° from the amino nitrogen and 3.22A° from carboxylic oxygen O_2A. The hydroxyl oxygen of molecule B is 2.91A° from the amino nitrogen and 3.22A° from the carboxylic oxygen O_2B.

TABLE 5

Hydrogen Bond Distances and Angles and van der Waals' Interactions of Less Than 3.50A

(A) Hydrogen Bond Distances and Angles

Donor	Acceptor	Dist.A°	Angle, degrees
N(A)	O_1A'	2.99	C_2A N(A) O_1A 120
N(A)	O_2A''	3.01	C_2A N(A) O_2A 91
N(B)	O_3B'''	2.95	C_2B N(B) O_3B 91
N(B)	O_2B''	2.99	C_2B N(B) O_2B 129
O_3A	O_1B'	2.70	C_3A O_3A O_1B 121
O_3B	O_3A'''	2.74	C_3B O_3B O_3A 99

(B) van der Waals' Interactions

Atoms	Distance
N(A).....O_1B''	3.44
C_2A.....O_1B''	3.36
O_2A'.....C_2B	3.27
C_1B.....O_2A'	3.39
C_2A.....O_2A''	3.40
N(A).....C_1A'	3.44
C_2B.....O_3B'''	3.32
C_3A''.....C_3B'''	3.48
C_3B.....O_3A'''	3.29
O_3A.....O_1A'	3.33

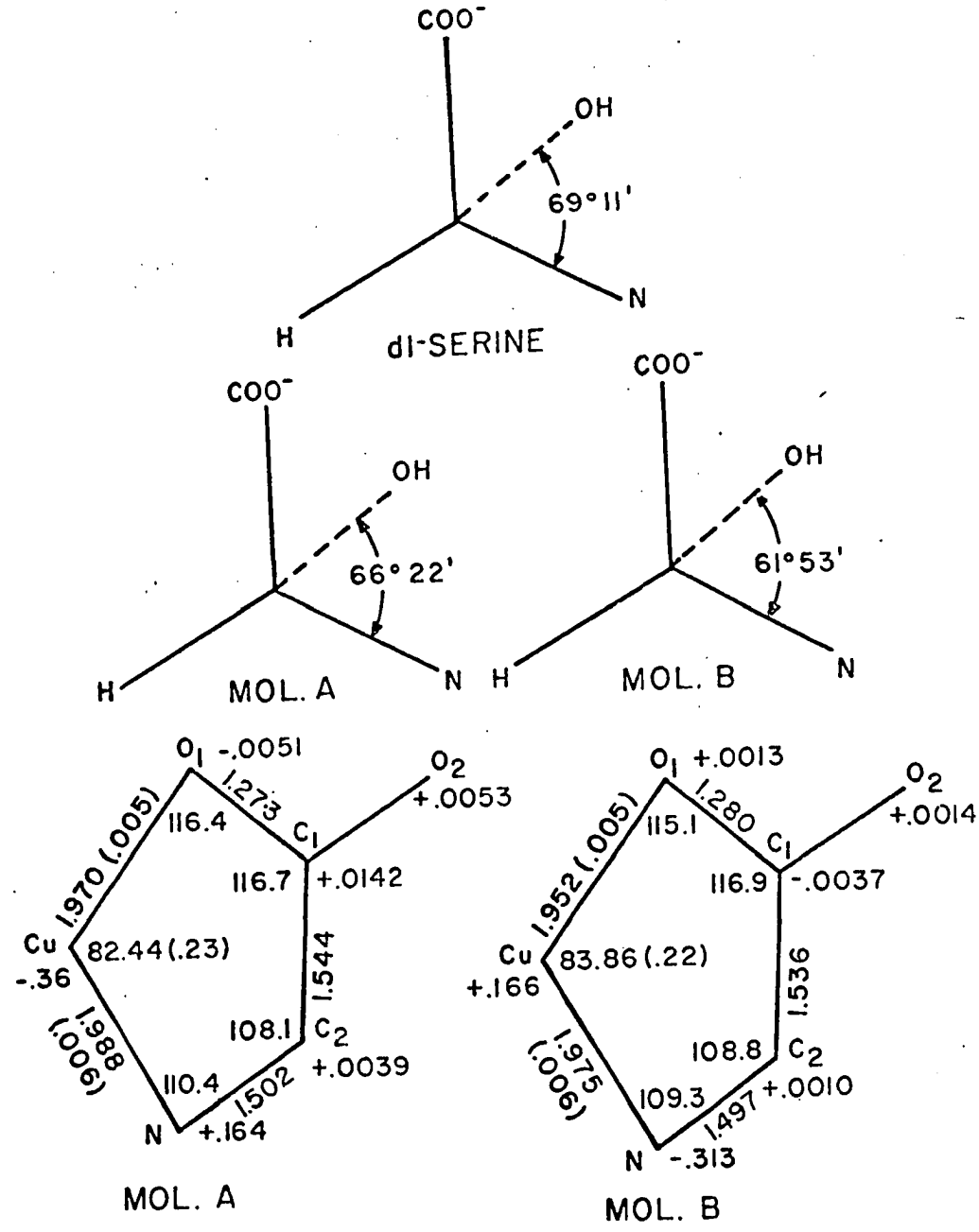

Figure 5. Configuration of l-Serine Molecules A and B and dl-Serine (Shoemaker, et al, 1953). Configuration of Chelate Rings of Mol. A and B.

Intramolecular bond distances and angles for both A and B molecules are given in Table 6 and Figures 6a and 6b. The values show a good consistency for the two l-serine molecules. One is tempted to suggest that an increase in length has occurred for the C_1-C_2 bond and a decrease in length for the C_2-C_3 bond. However, the differences from a normal C-C bond of 1.53A° and similar compounds listed in Table 7 is not significant. The bond distances within the carboxyl group suggests that more charge is on the ligand oxygen closest coordinated to copper. The C_1-O_1 bonds of length 1.273° and 1.280A° and the C_1-O_2 bonds of length 1.243 and 1.231 are similar to those found in the two carboxylic groups of copper glutamate dihydrate (8). These bond lengths approach the values found in carboxylic acids and reflect the fact that the longer bonds, C_1-O_1, are strongly bonded to the copper atom. The bonds involving the hydrogen atoms are reasonable. The normal bond distances are O-H, .95A°, C-H, 1.09A°, and N-H, 0.99A°. The largest deviations from these values are 0.24A° which occurred for C_3-H_1 (mol. B) and N-H (mol. B). The bond angles for both molecules were consistent with each other and in the expected range except for one angle. The angle C_3 C_2 N is 4.6° larger than a normal tetrahedral angle of 109°20', and 2.6° larger than the same angle in dl-serine (see Table 7). These differences are greater than 3σ and fall in the significant range. However, no

TABLE 6

Intramolecular Bond Angles and Distances

Bond		Molecule A	Molecule B
Bond Distances			
C_1	C_2	1.544(.010)	1.536(0.010)
C_2	C_3	1.507(.009)	1.497(.010)
C_2	N	1.502(.009)	1.484(.009)
C_1	O_1	1.273(.009)	1.280(.008)
C_1	O_2	1.243(.009)	1.231(.009)
C_3	O_3	1.410(.009)	1.412(.010)
C_2	H	1.04	1.14
C_3	H	1.14	0.85
C_3	H_2	1.04	1.04
N	H_1	0.79	0.75
N	H_2	0.91	1.09
O_3	H	———	0.84
Bond Angles			
O_1 C_1	O_2	125.2(.7)	123.4(.7)
O_1 C_1	C_2	116.7(.6)	116.9(.6)
O_2 C_1	C_2	118.1(.6)	119.6(.6)
C_1 C_2	N	108.2(.5)	108.8(.6)
C_1 C_2	C_3	110.5(.5)	112.8(.6)
C_3 C_2	N	113.3(.6)	113.9(.6)
C_2 C_3	O_3	109.6(.5)	109.4(.6)

Figure 6a. Intramolecular Bond Distances of bis(1-Serinato) Cu(II).

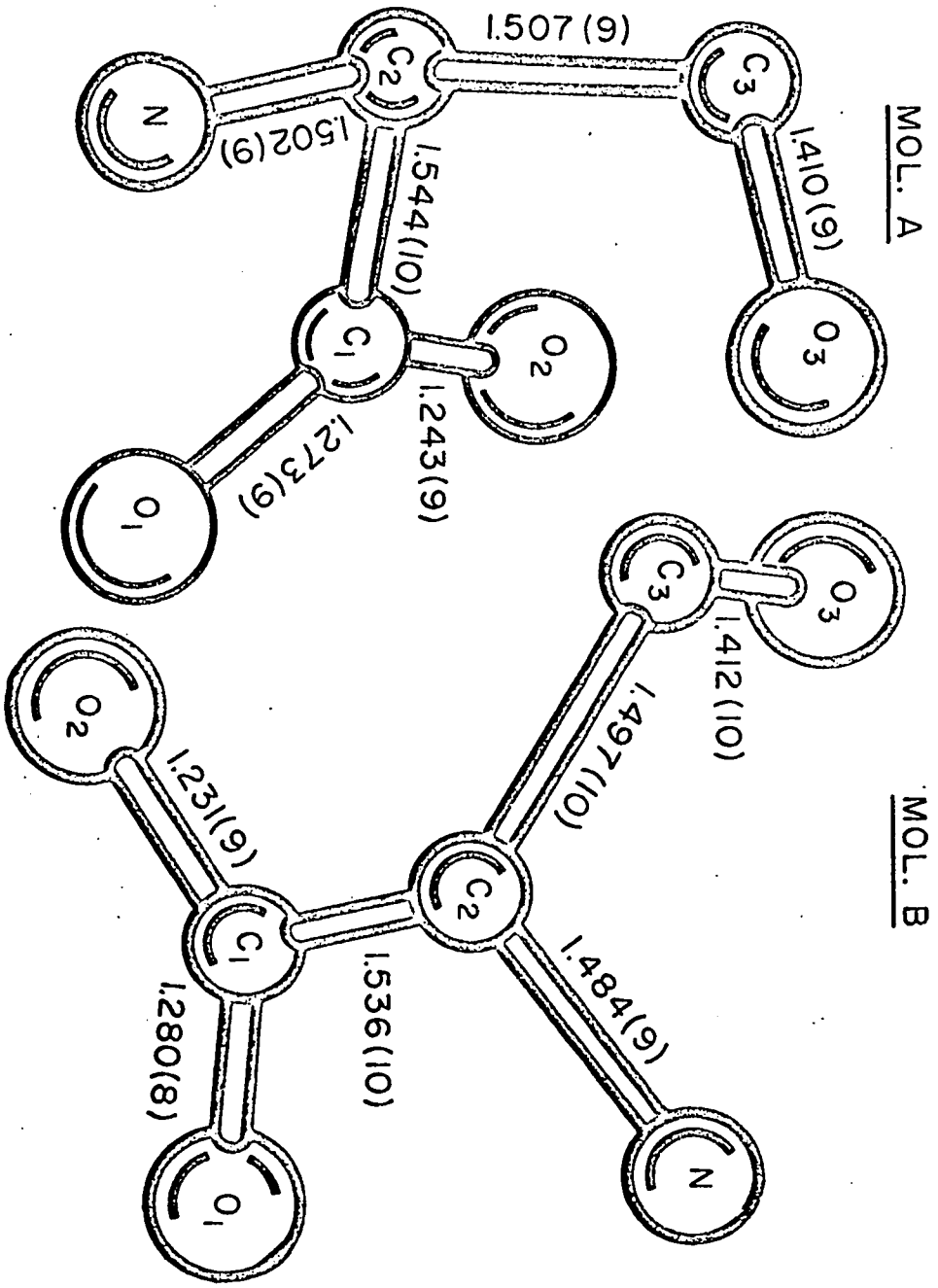

Figure 6b. Intramolecular Bond Angles of bis(l-Serinato) Cu(II).

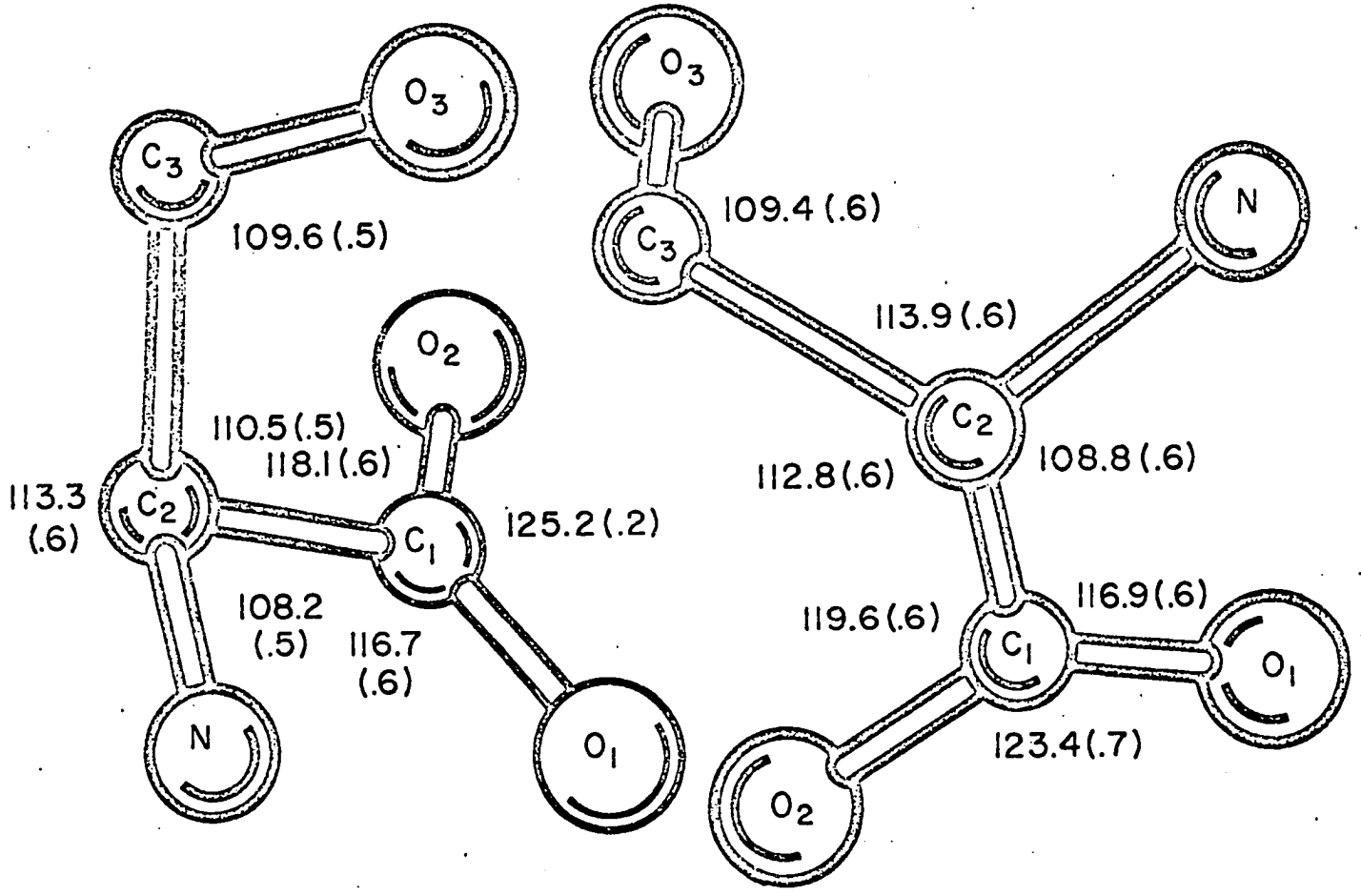

TABLE 7

Comparison of Bond Angles and Lengths of bis(l-Serinato) Cu(II) with Those of dl-Serine and other Copper Complexes of Amino Acids and Peptides

Bond	dl-serine	Complex*	Ave. Values of Cu Complexes[2]
Bond Distances			
C_1 C_2	1.528(.005)	1.540(.010)	1.52(.02)
C_2 C_3	1.513(.005)	1.502(.010)	1.53(.02)
C_2 N	1.491(.005)	1.493(.009)	1.48(.007)
C_1 O_1	1.268(.005)	1.277(.009)	1.27(.007)
C_1 O_2	1.261(.005)	1.237(.009)	1.23(.005)
C_3 O_3	1.425(.005)	1.411(.010)	
Bond Angles			
$O_1C_1O_2$	125.3	124.3(.7)	122.5
$O_1C_1C_2$	117.4	116.8(.6)	117.5
$O_2C_1C_2$	117.2	118.8(.6)	120.0
C_1C_2N	110.0	108.5(.6)	———
$C_1C_2C_3$	110.3	111.7(.6)	———
C_3C_2N	111.1	113.6(.6)	———
$C_2C_3O_3$	112.0	109.5(.6)	———

*Average bond lengths of molecules A and B.

general conclusions can be formed regarding this angle in relation to chelation. The averages of the bond lengths and angles of molecules A and B are given in Table 7 and compared with average values obtained from a large number of reported copper complexes of amino acids and peptides (2) and with the results of dl-serine (1). The shortening of the C=O bond and the lengthening of the C-O bond of the carboxyl group in the chelated l-serine appears to be the largest difference in bond lengths between the complexed and "free" dl-serine molecules. The bond angle $C_3\ C_2\ N$ is much larger in the chelated l-serine as was previously described. This comparison illustrates that small changes do occur in bond distances and angles between chelated and unchelated l-serine molecules.

The coordination configuration surrounding the copper ion is shown in Figure 7. The four ligand atoms of the two l-serine molecules, O_1A, N(A), O_1B, and N(B) lie at the corners of an approximately square pyramid. The square pyramid is completed by the carboxylic oxygen O_1A' of a symmetry related molecule. The closest approach of a neighboring atom to the 6th coordination position of the copper ion is 3.63A° for carboxylic oxygen O_2B''. The four closest ligand atoms are coordinated cis with respect to each other. The bond lengths from copper to the four closest ligand atoms are in the expected range. The two $Cu-NH_2$ bond lengths are slightly longer than the Cu-O bonds.

Figure 7. Coordination Sphere of Copper Ion in bis (l-Serinato) Cu(II).

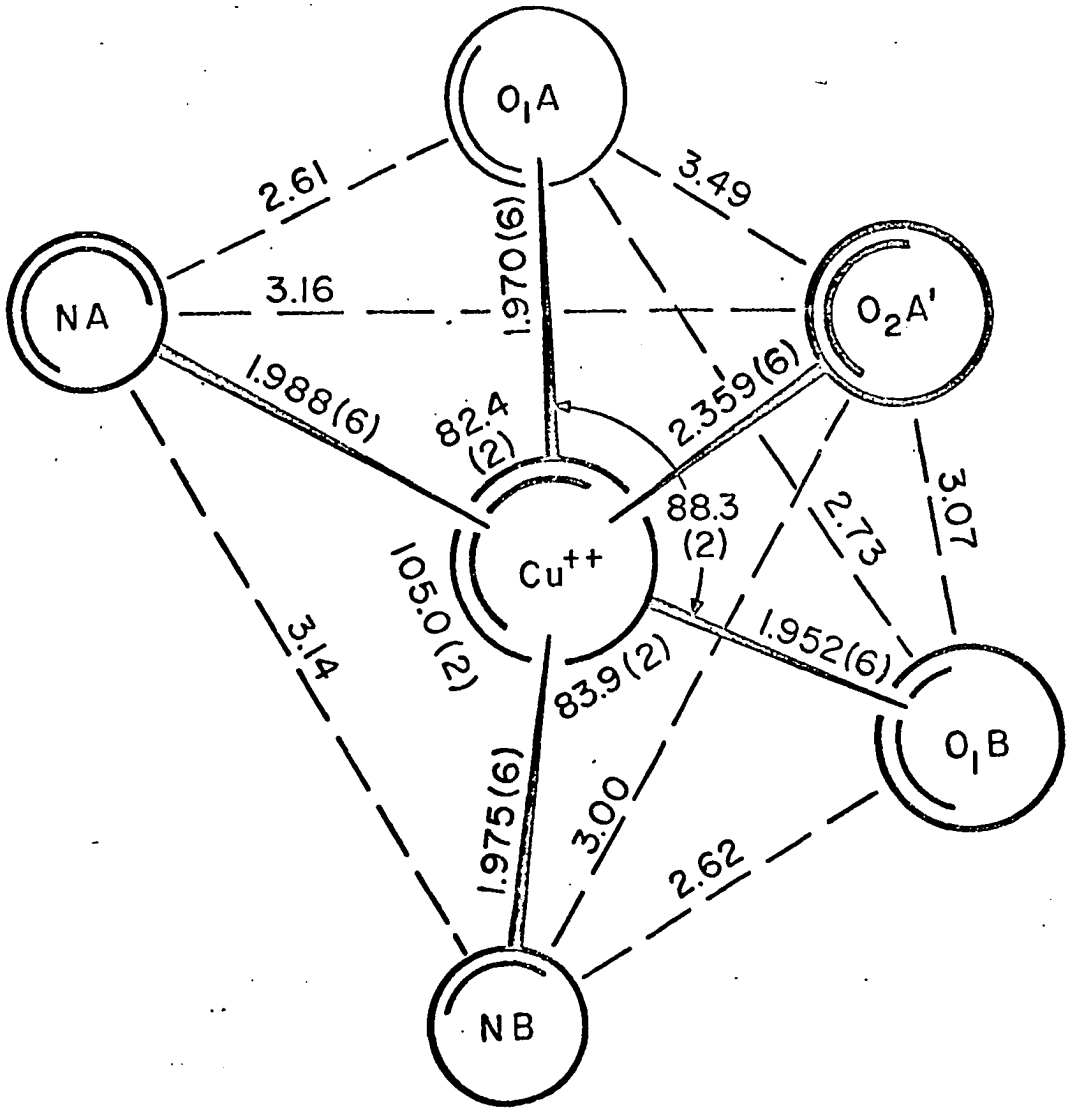

The copper ligand bond distances are in close agreement with average values of 1.99A° for Cu-NH_2 and 1.97A° for Cu-O bonds obtained from several copper complexes of amino acids and peptides (2). The sides of the square formed by atoms N and O_1 from the same molecule are 2.61A° and 2.62A° for A and B respectively. The remaining two sides are of length 3.14A° for N(A) and N(B) and 2.73A° for O_1A and O_1B. The difference in length of the sides points out the deviation from a regular square planar arrangement. This is further brought out in the deviation of the angles from the normal value of 90°. The value of 105° for the angle N(A) Cu N(B) is quite large and indicates considerable distortion around the copper ion. The least squares planes are shown in Table 8. Plane 1 calculated with Cu, O_1B, O_1A, O_1B, N(B), and N(A) show an average displacement of 0.10A°. Plane 2 calculated with only the four closest ligand atoms show an average deviation of 0.11A°. The copper ion was displaced toward the apex atom O_1A'. The displacement of ligand atoms along the diagonal in the same direction from the least square planes confers on the coordination square the shape of a flattened tetrahedron.

Bis glycinato copper (II) hydrate (3) is the only previously known example whose ligand atoms are coordinated cis with respect to each other. The coordination surrounding the copper ion in this complex is much less distorted

TABLE 8

Least Squares Planes for Coordination Sphere

Plane 1. O_1A, O_1B, N(A), N(B), Cu

Eqn. $4.07X + 5.86Y + 3.30Z = 5.72$

Plane 2. O_1A, O_1B, N(A), N(B)

Eqn. $4.07X + 5.87Y + 3.29Z = 5.69$

Atom	Dev. Plane 1	Dev. Plane 2
Cu	0.11	0.14
O_1A	-0.14	-0.12
O_1B	0.09	0.12
N(B)	-0.13	-0.10
N(A)	0.07	0.10
O_2A'	2.44	2.46

than what was observed for the copper chelate of l-serine. The average deviation of atoms from plane 2 for the glycine complex was 0.0325A° compared with 0.11A° found for the l-serine complex. The sides completed by the two nitrogen atoms (2.98A°) and the two oxygen atoms (2.83A°) of the glycine complex differ by 0.15A° whereas for the l-serine complex the difference is 0.41A°.

The configuration of the two five membered chelate rings are shown in Figure 5. The carboxylic groups consisting of atoms C_1, O_1, O_2, and C_2 are planar. The copper atom is displaced -0.36A° from the carboxylic group of molecule A and 0.17A° from the plane of the carboxylic group of molecule B. The nitrogen atom of each molecule is not in the plane of the carboxylic group. Nitrogen atom N(A) is displaced 0.16A° and N(B) displaced -0.31A° from the carboxyl group of molecules A and B respectively. The displacement of copper and nitrogen atoms from the planes of the carboxylic groups illustrates that both rings are "buckled" in opposite directions. In dl-serine, the nitrogen atom is reported (1) to be in the plane of the carboxyl group, but in chelated l-serine molecules A and B the nitrogen atoms are out of the plane of the carboxylic groups. In chelation of l-serine, a rotation around the bond C_1-C_2 has occurred which is the largest difference occurring when the l-serine molecules interact with copper (II) ions. The planes of the carboxylic groups are

summarized in Table 9.

TABLE 9

Least Squares Plane for Carboxylic Groups

O_1, O_2, C_1, C_2

Molecule A Equation. $7.14X + 4.81Y + 2.12Z = 6.09$

Molecule B Equation. $5.28X + 5.53Y + 2.98Z = 5.73$

Atom	Dev. Mol. A	Dev. Mol. B
O_1	-0.005	0.001
O_2	-0.005	0.001
C_1	0.014	-0.004
C_2	-0.004	0.001
N	0.164	-0.313
Cu	-0.360	0.166

Principal axes of the anisotropic ellipsoids are shown in Table 10 along with the direction cosines. The thermal motion was largest for atom O_2B. This atom, however, is involved in only one weak hydrogen bond and no intermolecular interactions less than 3.50A°. The B value of 4.07 obtained for O_1A is much larger than the B values of the other atoms comprising the coordination square, and is probably due to this atom occupying the fifth position around the copper ion.

TABLE 10

Principal Axes and Direction Cosines of Anisotropic Ellipsoids

Atoms	B	l_1	l_2	l_3
Cu	2.20	.539	.464	.697
	1.25	.777	.047	-.636
	1.04	-.324	.884	.332
O_1B	2.95	.639	.510	.569
	1.75	.756	-.280	-.600
	1.27	-.141	.813	-.563
O_1A	4.07	.666	.604	.431
	1.43	-.226	-.397	.892
	1.13	-.711	.691	.136
N(B)	2.25	.829	.330	.442
	1.35	-.485	.024	.879
	0.89	-.278	.944	-.177
N(A)	1.90	.941	.001	-.350
	1.51	.333	.198	.918
	0.98	-.068	.980	-.185
O_2A	2.75	.884	.403	.225
	1.83	-.212	-.102	.974
	1.24	-.416	.909	.009
C_1B	3.07	.580	-.508	.631
	1.93	-.068	.749	.659
	1.01	.812	.425	-.409
C_2B	2.14	.794	.268	.537
	1.97	-.186	.962	-.199
	0.96	-.579	.058	.820
C_3B	2.98	.711	-.394	.574
	2.00	-.699	-.304	.655
	1.45	.078	.867	.491
O_3B	4.14	-.620	.121	.782
	1.94	.753	-.184	.623
	1.75	.219	.975	.021
O_2B	4.58	.792	.391	.460
	2.89	-.473	.879	.071
	1.32	-.386	-.274	.885

TABLE 10--Continued

Atoms	B	l_1	l_2	l_3
C_1A	2.28	-.020	.037	.999
	1.57	.620	.784	-.023
	0.80	.784	-.619	.030
C_2A	1.72	.846	.383	.361
	1.47	-.475	.858	.203
	1.24	-.242	-.343	.910
C_3A	2.68	.656	-.124	.738
	1.79	.608	-.498	-.625
	1.34	.448	.858	-.256
O_3A	3.64	-.550	.365	.757
	2.74	-.427	.649	-.624
	1.26	.717	.668	.192

CHAPTER III

CRYSTAL AND MOLECULAR STRUCTURE ANALYSIS OF THE COPPER CHELATE OF GLYCYL-1-LEUCYL-1-TYROSINE

Experimental Results

1. Crystallization Procedure.

Crystals of the copper complex of glycyl-l-leucyl-l-tyrosine, Cuglt, were obtained using three similar methods.

Method 1.--$2CuSO_4 + 2Ba(OH)_2 + glt \rightarrow 2BaSO_4 + Cuglt + Cu(OH)_2 + 2H_2O$. The Chelate solution, approximately 0.031M in peptide, was filtered to remove $BaSO_4$ and $Cu(OH)_2$ and evaporated to dryness at room temperature in a 10 ml beaker. The 10 ml beaker containing the complex dissolved in water and ethanol was placed in a 200-300 ml screw-cap jar that contained 3 to 5 ml of ether. The level of ether had to be lower than the height of the 10 ml beaker to insure that ether would not spill into the beaker. The jar was tightly sealed with a screw cap and the chelate solution and ether were allowed to equilibrate at room temperature. Crystals normally appeared on standing overnight.

Method 2.--$CuSO_4 + Ba(OH)_2 + glt \rightarrow BaSO_4 + Cuglt + 2H_2O$. The chelate solution which was approximately 0.055M

in peptide was equilibrated with ether after filtering $BaSO_4$. Crystals of varying sizes appeared on standing overnight.

Method 3.--$CuCl_2$ + glt$\longrightarrow$Cuglt + 2HCl. A quantity of 0.0553 gms. of $CuCl_2$ and 0.0589 gms. of peptide was weighed on an analytical balance. The two solids were diluted to 3.00 ml with H_2O. The chelate solution was passed through a ¾" diameter chromatographic column containing 30.00 gms. of Bio-Rad analytical grade ion exchange resin AG11A850-100 mesh. The blue eluate from the column was evaporated to dryness. The blue residue was redissolved in 0.5 ml of H_2O and equilibrated with ether. Nice large blue crystals appeared overnight. The pH of the chelate solutions used in methods 1 and 2 had values from 6 to 7. Method 2 was the most consistent in yielding crystals. Neither of the three methods, however, yielded crystals each time it was used.

The crystals of Cuglt were blue plates. The plates were usually well formed. The crystals decomposed very rapidly ($<$60 Secs.) on exposure to the atmosphere. Decomposition could be stopped by keeping the crystals in the "mother liquor" enclosed in an environment of ether. The density of the crystals was estimated as 1.49 by the flotation method. No accurate determination of the density was possible due to the fact that the crystals decomposed rapidly in a foreign environment. The ratio of copper to

peptide in the chelate solution was determined as 1 mole of copper to 1 mole of peptide by means of an edta titration.

2. Determination of Crystal Properties.

The rapid decomposition of the crystal in a foreign environment made it necessary to find a way in which x-ray data could be obtained while keeping the crystal in its original environment. This problem was solved by using specially made tapered glass capillaries of 0.5 mm diameter, and 0.01 mm wall thickness. The capillary was opened on both ends, filled completely with the mother liquor, and resealed at the end that was broken with a flame from a micro-jet burner. Using a spatula and a pin point probe, the crystal was transferred from the "mother liquor" in the beaker to the "mother liquor" in the capillary. The crystal was secured in the capillary by forcing it down the tapered capillary with a tiny glass rod until a diameter of the capillary was reached that was smaller than the width of the crystal. This method secured the crystal quite well in the capillary. The height of the crystal from the bottom of the capillary was shortened if necessary by breaking the capillary at the sealed end at the approximate distance needed from the crystal and then resealing. A height of between 10 mm to 20 mm of the crystal from the end of the capillary was necessary for final adjustment using the goniometer. The level of the

"mother liquor" in the capillary was lowered to 5 to 10 mm above the crystal, and a layer of ether 2-4 mm length was placed on top of the "mother liquor." The top of the capillary was sealed with a small flame from a micro-jet burner. Immersing the capillary in a beaker of ice water reduced the vapor pressure of ether, and sealing of the capillary was much easier. The capillary containing the crystal was sealed on the goniometer with clay. The crystal was now ready for optical and x-ray examination.

The goniometer containing the capillary with the crystal was mounted on an X-RD5 General Electric diffractometer. The intensities of several reflections recorded over an interval of two to three days did not change. Three mutually perpendicular axes were found for the crystal. The space group of the crystal was determined by plotting the reflections found in the h0l, hk0, and 0kl planes. Systematic extinctions occurring were h00, 0k0, 00l where h, k, and l were odd. The only space group showing these extinctions in the International Tables for x-ray crystallography Vol. 1 is $P2_12_12_1$. This space group is unambiguously determined. The cell dimensions were determined by the method of least squares with 49 reflections. Using the estimated density of 1.49, the molecular weight of a 1:1 complex, the number of molecules in the unit cell was calculated as 11. However, it was assumed there were 8 molecules in the unit cell or two moles of copper and

two molecules of peptide in the asymmetric unit. The complete composition of the complex was unknown until the structure had been solved. The molecular formula of the complex obtained from a solution of the structure was Cu_2(glycyl-l-leucyl-l-tyrosine)$_2$ $8H_2O \cdot C_2H_5OC_2H_5$. The asymmetric unit contained two moles of copper, two molecules of peptide, 8 molecules of water, and one molecule of ether. The crystal properties of the complex are summarized in Table 1.

TABLE 1

Crystal Properties of Cu_2(gly-l-leu-l-tyr)$_2$ $8H_2O \cdot Et_2O$

Space Group	$P2_12_12_1$
No. of Molecule in Unit Cell	4
Cell Dimensions	a = 9.316(.002)
	b = 25,764(.001)
	c = 21.046(.001)
	$\alpha = \beta = \gamma =$ 90°
Density	
	est. = 1.49
	calc. = 1.37
F(000)	2192
Molecular Formula:	$Cu_2(C_{17}H_{25}N_3O_5)_2 \cdot 8H_2O \cdot C_4H_{10}O$
Molecular Weight	1044.12
Mosaic Spread	0.1°
Volume	5051A°(3)

3. Collection of Intensity Data.

The mosaic of the crystals was determined as 0.1°. Integrated intensities were collected out to a 2θ value of 90° using a theta-2θ scan. Minitor values were taken every 30 to 50 reflections. CuKα radiation was used to measure 2043 observed reflections and 311 unobserved reflections. Three crystals were used to collect the data. Absorption and Lorentz-Polarization corrections were applied to the data.

4. Determination and Refinement of Trial Structure.

a. Interpretation of the Patterson Map.

The Patterson map was calculated for one-eighth the unit cell on a grid of approximately $0.2A^{\circ}$ for each grid point. The Patterson function was sharpened as previously described for bis(l-serinato) Cu(II). Sections were computed perpendicular to the b axis. The equivalent positions for space group $P2_12_12_1$ are

x	y	z	(1)
½-x	$\bar{y}$	½+z	(2)
½+x	½-y	$\bar{z}$	(3)
$\bar{x}$	½+y	½-z	(4)

which give rise to three Harker peaks in the Patterson map for each copper ion. The location of these peaks are defined by vectors with components (UVW) in the Patterson map and also in real space by the components (x,y,z)

U	V	W	
½-2x	2y	½	(5a)
½	½-2y	2z	(5b)
2x	½	½-2z	(5c)

Four additional peaks also occur in the Patterson map due to interactions between non-symmetry related copper ions. These vectors, (UVW) in the Patterson map, are defined by the components (x,y,z) in real space as

U	V	W	
x_2-x_1	y_2-y_1	z_2-z_1	(6a)
$½-x_2-x_1$	$-y_2-y_1$	$½+z_2-z_1$	(6b)
$½+x_2-x_1$	$½-y_2-y_1$	$-z_2-z_1$	(6c)
$-x_2-x_1$	$½+y_2-y_1$	$½-z_2-z_1$	(6d)

The relative peak height of each of the heavy atom vectors in the Patterson map is 729. The symmetry of the Patterson map for space group $P2_12_12_1$ is P2/m2/m2/m. The equivalent positions for P2/m2/m2/m are

$$U,V,W;\ \overline{U},\overline{V},W;\ U,\overline{V},\overline{W};\ \overline{U},V,\overline{W}$$
$$\overline{U},\overline{V},\overline{W};\ U,V,\overline{W};\ \overline{U},V,W;\ U,\overline{V},W$$

and the translation equivalent positions.

In Table 2 are listed the six Harker peaks and four general peaks due to heavy atom vectors in the Patterson map. Vectors 1 through 3 were assigned as the Harker peaks for Cu(1), and vectors 4 through 6 were assigned as the Harker peaks

TABLE 2

Peaks due to Heavy Atom Vectors in Patterson Map

Peak No.	Components in Real Space			Components in Vector Space			Peak Height	Type of Peak
1	½	½-2y_1	2z_1	½	44	14	617	Harker
2	2x_1	½	½-2z_1	34	½	36	419	Harker
3	½-2x_1	2y_1	½	16	06	½	457	Harker
4	½	½-2y_2	2z_2	½	32	30	567	Harker
5	2x_2	½	½-2z_2	22	½	20	606	Harker
6	½-2x_2	2y_2	½	30	18	½	472	Harker
7	Equation (6)			22	6	22	469	general
8	Equation (6)			8	12	28	501	general
9	Equation (6)			28	38	8	484	general
10	Equation (6)			42	44	42	476	general

for Cu(2). The coordinates of one of the copper atoms can be determined by choosing either of the 8 equivalent positions in space group P2/m2/m2/m. The equivalent position $\bar{U},V,W$ was chosen for Cu(1), and utilizing equations 5a, 5b, and 5c, the coordinates ($x_1y_1z_1$) in real space for Cu(1) were determined as

0.33 0.03 0.07

respectively. The origin of real space has now been defined relative to Cu(1). Therefore, the coordinates ($x_2y_2z_2$) of Cu(2) have to be chosen with respect to this origin. In

other words the coordinates for Cu(2) must not only satisfy the vectors due to Harker peaks but also must satisfy the four general vectors 7 through 10 with the above coordinates of Cu(1). There is only one set of coordinates of Cu(2) that will satisfy both of these conditions simultaneously. The eight solutions of the Patterson map for Cu(2) are obtainable from different combinations of $x_2y_2z_2$ where

x_2	y_2	z_2
$\pm$0.11	$\pm$0.09	$\pm$0.15.

The only coordinates ($x_2y_2z_2$) of Cu(2) obtained from the Harker peaks that satisfy the four general vectors in the Patterson map when used with the coordinates of Cu(1) are

0.11	0.09	-0.15

respectively for ($x_2y_2z_2$). The coordinates of Cu(2) are now defined with respect to the same origin as Cu(1). The origin of $P2_12_12_1$ is located mid-way between the three non-intersecting screw-axes. A new set of coordinates could be determined for Cu(1) and Cu(2) by defining a new origin with the above condition. The coordinates of the two copper ions in the asymmetric unit as determined from the Patterson map were

	x	y	z
Cu(1)	0.33	0.03	0.07
Cu(2)	0.11	0.09	-0.15.

A complete map of real space was determined from vector space (Patterson map) by utilizing the superposition method (17). The superposition method constitutes a way in which the fundamental set (real space) can be recovered from the vector set (Patterson Space). The superposition method as applied by Beevers and Robertson (19) was used in this work. This application assumes the position of the heavy atoms in the unit cell to be known. The Patterson function is then set down with its origin at each of the known atomic positions. The images of other atoms in each of the known heavy atoms are brought into coincidence on atomic sites. In applying this method to Cu_2(gly-l-leu-l-tyr)$_2 \cdot 8H_2O \cdot Et_2O$ the origin of the Patterson map was placed in turn on the eight atomic positions of the copper ions occurring in space group $P2_12_12_1$. Eight superpositions were then possible. This procedure was carried out using an IBM 1620 computer program that systematically checked combinations of xyz in real space for x=0 to x=50, y=0 to y=100, and z=0 to z=50 to ascertain those locations in real space where eight coincidences occurred. The minimum value of the Patterson function resulting from the eight superpositions was used to define the peak height at each location in real space.

A second map of real space (electron density map) was computed by utilizing the observed amplitudes and phases calculated from the two copper positions in a

Fourier summation. Peaks that were present in both maps of real space were taken as corresponding to atomic positions. The peak heights in the map obtained from the superposition method ranged from 0 to a maximum of 200 for the copper positions. A model was constructed from the coordinates of peaks that were present in both maps.

b. Interpretation of the Maps of Real Space.

The configuration around the copper atoms was quite ambiguous. More than six peaks occurred around each copper atom at distances of less than 3.0A°. Since copper is known to have coordination numbers of 4, 5, or 6 in amino acids and peptide complexes, some of the peaks were either spurious or were due to carbon atoms bonded to ligand atoms. All attempts to resolve the configuration around the copper atoms were futile. Our efforts were then directed toward finding the two benzene rings with the idea that the location of the rings could be used as a starting point for isolating the remaining part of the molecule. Two sets of atoms that corresponded to the geometry of a benzene ring were located at favorable positions with respect to the copper atoms. Their locations were such that each ring was closer to one copper atom than the other. This led to the belief that one molecule was bonded to the copper atom close to the benzene ring via the carboxyl group at one end and to the second copper atom farthest removed from the benzene ring via the terminal nitrogen atom.

In other words the complex was a dimer as opposed to one molecule being coiled or wrapped around one copper atom. Using the above considerations it was only a matter of time before a trial structure was deduced.

The atoms comprising the peptide chain were located with varying degrees of confidence. Two carbon atoms of the isopropyl group and one carbon atom of a benzene ring were not found in either map. The peaks of some water molecules were present in both maps. A structure factor calculation was made with only the atoms of the peptide molecules that were located and the two copper atoms. The trial structure obtained from the two maps gave an R-Index of 31.5%.

c. Refinement of Trial Structure and Location of Remaining Atoms from Difference Synthesis.

The trial structure was refined by three dimensional block diagonal least squares and the same weighting scheme used for bis(l-serinato) Cu(II) with P_1 assigned the value of 41 and with anisotropic copper atoms and isotropic light atoms. After several cycles of least squares refinement, R-Index of 17.0%, a difference map was calculated. Seven water molecules and the remaining three carbon atoms were present in the difference map. Also, four additional peaks were present in the Fourier whose configuration, separation distances, and their location in the unit cell did not correspond to water molecules or part of the peptide molecules. We omitted these peaks from refinement cycles on the assumption that they would disappear as the structure

was refined with the above 10 additional atoms included in the refinement cycles. The structure was further refined to an R-Index of 12.5%. At this stage of the refinement one of the methyl carbon atoms of the isopropyl group had a large isotropic temperature factor and a bond distance to the tertiary carbon atom of 1.85A°. A second difference map was calculated with this isopropyl atom omitted from the structure factor calculation for obtaining the phases to compute the difference map. The location of the isopropyl atom in the second difference map was the same location obtained from least squares. Also, the atom showed no disorder in the difference map. The four peaks mentioned earlier were also present in this second difference map. Furthermore, a fifth peak in close proximity to the four peaks was resolved in this second map that could not be observed in the first difference map. The configuration of the five peaks are given below.

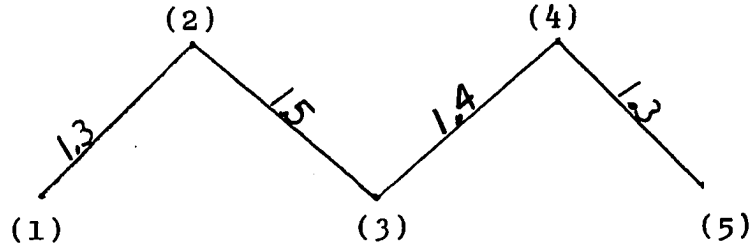

The peak heights of these five peaks along with that of the isopropyl carbon atom in the difference map on an absolute electron density scale were

Peak No.	Peak Height $e/(A^{\circ})^3$
(1)	1.26
(2)	1.30
(3)	2.10
(4)	1.39
(5)	1.29
Isopropyl carbon atom	1.27

The similarity of the peak heights of peaks 1, 2, 4, and 5 to the peak height of the isopropyl carbon atom indicated that these four peaks were carbon atoms, and the largest peak was probably an oxygen. Moreover, the geometry of the five peaks indicated an organic residue. Recalling that the complex was crystallized by equilibrating with ether, then the most obvious explanation was that these peaks were due to a molecule of ether. To help substantiate this idea, the distances of the atoms of the ether molecule from other atoms within one unit cell and neighboring unit cells were computed. These computations showed the oxygen atom, peak #3, to be separated at a hydrogen bond distance from a water molecule. Secondly, one of the carbon atoms was within van der Waals' distance of two of the carbon atoms from a benzene ring which was the only short van der Waals' distance for the five peaks. Therefore, the packing of the molecule within the unit cell was consistent with the properties of ether. It forms one hydrogen bond furnishing the acceptor atom and packs close to groups of

similar polarity. One further peak appeared in the second difference map with a height of $0.97e/(A^{o})^{3}$. The location of this peak in the unit cell was favorable for a water molecule, but since the peak height was low (compare with $2.0e/(A^{o})^{3}$ for oxygen peak #3) it was omitted at the present from least squares refinement. Isopropyl carbon atom and the carbon atoms and oxygen atom of the ether molecule were included in the next cycles of least squares. A third difference map was calculated after two cycles of refinement. There was a slight increase in peak height of the suspected water molecule from $0.97e/(A^{o})^{3}$ to $1.02e/(A^{o})^{3}$. This peak was included as a water molecule in subsequent least squares refinement. On refining this molecule isotropically, the isotropic value steadily increased to a value of 31.86. Furthermore, the z parameter continued to have positive shifts. A fourth difference map was computed which showed the presence of a smaller peak of height $0.81e/(A^{o})^{3}$. These two peaks, separated by $1.5A^{o}$ were found at the locations

	x	y	z	P.H.
$H_2O(1)$	0.085	-0.33	-0.0585	$0.94e/(A^{o})^{3}$
$H_2O(1)'$	0.080	-0.365	0.030	$0.81e/(A^{o})^{3}$

in the difference map. The peak for $H_2O(1)$ was elongated in the z direction toward $H_2O(1)'$. These two peaks were considered to be one disordered water molecules. They were included in further cycles with occupancy numbers of

2/3 for $H_2O(1)$ and 1/3 for $H_2O(1)'$ but not refined. The refinement was concluded when the shifts of the thermal and coordinate parameters were all less than 1/3 their standard deviations.

The numbering system of one peptide molecule and the ether molecule are shown in Figure 1. Table 3 lists the final atomic parameters along with their standard deviations. The observed amplitudes are listed in Table 4 along with their corresponding calculated values and phase angles. There were 2043 observed amplitudes that were used in the refinement cycles, and the 311 unobserved reflections listed in Table 2 of Appendix I were not included in least squares refinement. The exclusion of the unobserved reflections was an omission and the final atomic parameters do not necessarily account for the unobserved reflections. The final R-Index for all 2354 amplitudes was 0.108. The final R-Index for the 2043 observed amplitudes was 0.1030.

The final difference map contained only two spurious peaks previously mentioned. The estimated standard deviations are probably higher than those listed because of the large number of parameters, 270, that were refined utilizing 2043 pieces of intensity data. This is one reason for the errors obtained. The anisotropy of the light atoms which was not corrected, also contributes to the error, and finally the intensity data itself. Three

Figure 1. Numbering System for the Peptide and Ether Molecules

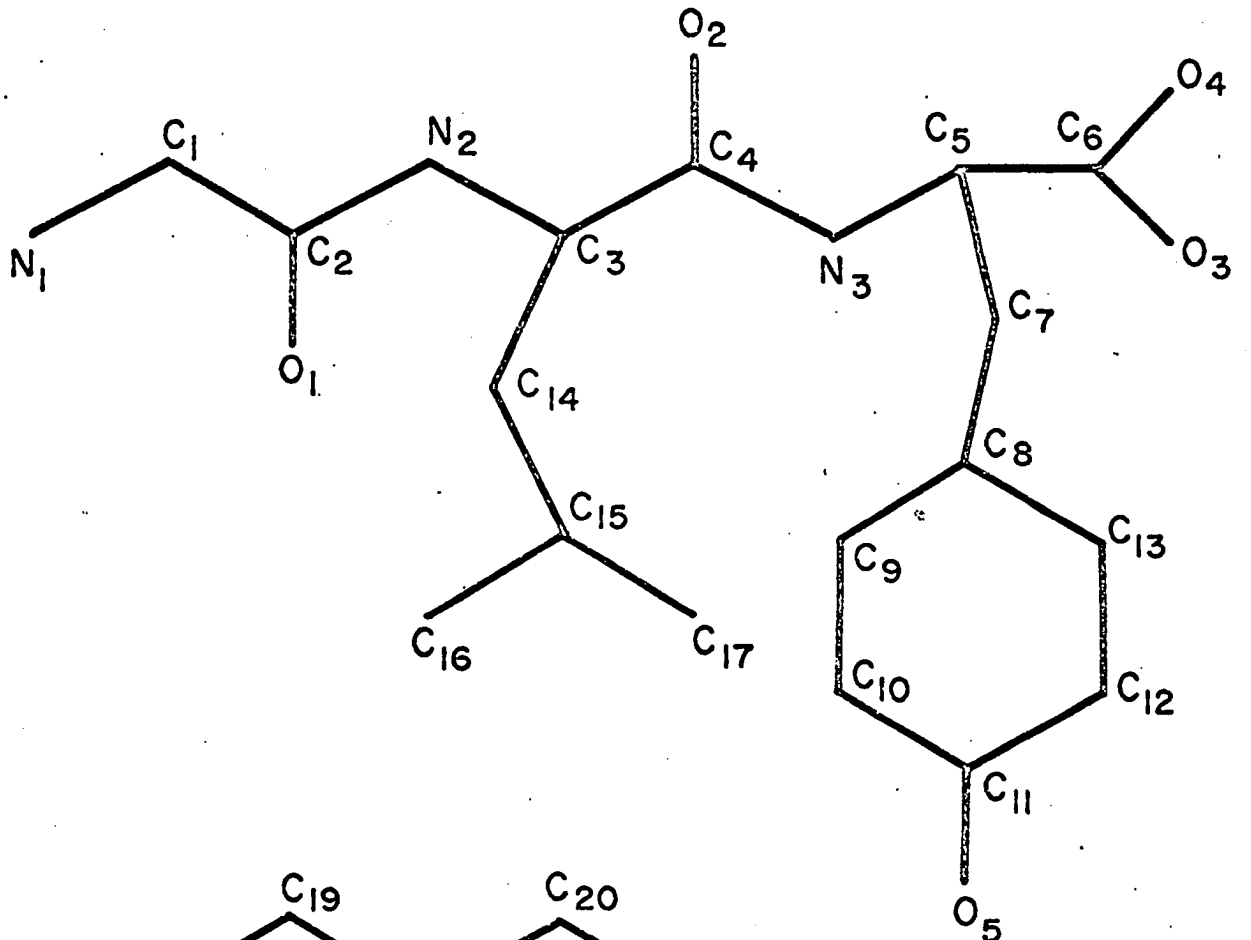

TABLE 3

Atomic Parameters of Cu_2(gly-l-leu-l-tyr)$_2$ $8H_2O \cdot Et_2O$

	Molecule A			
	X	Y	Z	Biso
N_1	.5248(20)	-.0409(8)	.0384(10)	5.95(50)
C_1	.6338(20)	-.0280(8)	.0847(9)	3.01(40)
C_2	.5662(20)	-.0133(7)	.1454(9)	2.24(40)
O_1	.4304(10)	-.0143(4)	.1505(6)	2.48(30)
N_2	.6514(20)	-.0004(6)	.1918(7)	3.04(90)
C_3	.5982(20)	.0099(7)	.2598(9)	2.72(40)
C_4	.6634(20)	.0611(7)	.2776(9)	2.34(40)
O_2	.7912(20)	.0714(6)	.2632(7)	4.21(30)
N_3	.5834(20)	.0934(6)	.3087(7)	3.12(30)
C_5	.6481(20)	.1423(9)	.3214(10)	4.08(50)
C_6	.5850(30)	.1627(10)	.3861(10)	5.37(60)
O_3	.4703(20)	.1442(6)	.4059(7)	4.59(40)
O_4	.6534(20)	.2013(7)	.4112(9)	7.59(50)
C_7	.6200(30)	.1859(10)	.2676(10)	6.02(60)
C_8	.4599(30)	.1923(10)	.2557(10)	6.03(70)
C_9	.3820(30)	.1611(10)	.2212(10)	5.23(60)
C_{10}	.2290(30)	.1669(10)	.2125(10)	6.16(70)
C_{11}	.1656(30)	.2039(10)	.2557(10)	6.97(70)
C_{12}	.2411(30)	.2371(10)	.2837(10)	7.48(80)
C_{13}	.3811(30)	.2313(10)	.2940(10)	7.04(70)
O_5	.0126(20)	.2047(8)	.2499(10)	8.22(50)
C_{14}	.6490(20)	-.0343(8)	.3033(9)	3.36(50)
C_{15}	.6107(30)	-.0900(10)	.2804(10)	4.03(50)
C_{16}	.4479(40)	-.0944(10)	.2847(20)	9.53(100)
C_{17}	.6827(40)	-.1284(10)	.3257(20)	8.62(90)

TABLE 3--Continued

	Molecule B			
	X	Y	Z	Biso
N_1	.1933(20)	.1112(6)	.3785(8)	3.67(40)
C_1	.0800(20)	.0862(8)	.3411(9)	3.11(40)
C_2	.1510(20)	.0491(7)	.2917(9)	2.85(40)
O_1	.2848(10)	.0420(5)	.2950(6)	3.27(30)
N_2	.0693(20)	.0264(6)	.2533(7)	2.93(40)
C_3	.1226(20)	-.0129(7)	.2052(8)	1.73(40)
C_4	.0568(20)	.0029(8)	.1412(10)	3.12(50)
O_2	-.0756(10)	.0169(5)	.1398(6)	3.09(30)
N_3	.1389(20)	-.0019(6)	.0901(7)	3.28(40)
C_5	.0664(20)	.0115(8)	.0303(10)	3.46(50)
C_6	.1216(20)	-.0278(8)	-.0181(9)	2.82(40)
O_3	.2433(20)	-.0506(6)	-.0083(7)	4.08(30)
O_4	.0592(10)	-.0308(6)	-.0706(7)	4.41(30)
C_7	.0915(30)	.0661(9)	.0087(10)	4.80(60)
C_8	.2588(30)	.0781(10)	-.0014(10)	4.68(60)
C_9	.3196(30)	.0634(10)	-.0609(10)	7.14(70)
C_{10}	.4673(30)	.0700(10)	-.0642(10)	7.07(70)
C_{11}	.5491(30)	.0854(10)	-.0211(10)	6.06(70)
C_{12}	.4979(30)	.0998(10)	.0369(10)	6.66(70)
C_{13}	.3357(30)	.0924(10)	.0448(10)	6.19(60)
O_5	.6972(30)	.0891(10)	-.0256(10)	11.28(70)
C_{14}	.0596(30)	-.0650(10)	.2309(10)	5.31(60)
C_{15}	.0921(40)	-.1104(10)	.1863(10)	7.80(80)
C_{16}	-.0309(40)	-.1197(10)	.1370(20)	9.99(100)
C_{17}	.0935(50)	-.1638(20)	.2347(20)	11.66(110)

TABLE 3--Continued

	X	Y	Z	Biso
		H_2O Molecules		
$H_2O(1)$*	.9174	.1590	.5372	31.86
$H_2O(2)$	.3243(30)	.1875(10)	.5034(10)	13.00(80)
$H_2O(3)$	.6403(40)	.2342(10)	.5413(10)	16.15(110)
$H_2O(4)$	.3196(30)	.3436(10)	.9638(10)	12.98(80)
$H_2O(5)$	-.2608(30)	-.0382(10)	-.0612(10)	12.28(80)
$H_2O(6)$	1.1440(40)	.1265(10)	.5918(20)	17.88(120)
$H_2O(7)$	.4304(30)	.2754(9)	.6182(10)	11.21(70)
$H_2O(8)$	.3898(30)	.3662(10)	.8398(10)	11.89(70)
$H_2O(1)'$*	.42	.365	.53	9.00
		Ether Molecule		
C_{18}	.1289(60)	.2406(20)	.8782(30)	17.43(180)
C_{19}	.1350(60)	.2132(20)	.9342(30)	17.85(180)
O_9	.1518(40)	.2504(10)	.9838(20)	15.40(100)
C_{20}	.1372(70)	.2327(20)	1.0393(30)	18.97(210)
C_{21}	.1032(70)	.2677(20)	1.0881(30)	17.69(180)
		Copper Ions		
Cu(1)	.3268(3)	-.0285(1)	.0721(1)	
Cu(2)	.3935(3)	.0911(1)	.3504(1)	

Anisotropic Values of Copper Ions

	b_{11}	b_{22}	b_{33}	b_{23}	b_{13}	b_{12}
Cu(1)	.0087(4)	.0031(1)	.0020(1)	.0008(1)	.0000(3)	.0006(3)
Cu(2)	.0094(3)	.0021(1)	.0021(1)	.0010(1)	.0002(3)	.0003(3)

*$H_2O(1)$ Disordered Water (2/3).

$H_2O(1)'$ Disordered Water (1/3).

TABLE 4

Amplitudes (X10) Along with Phase Angles.

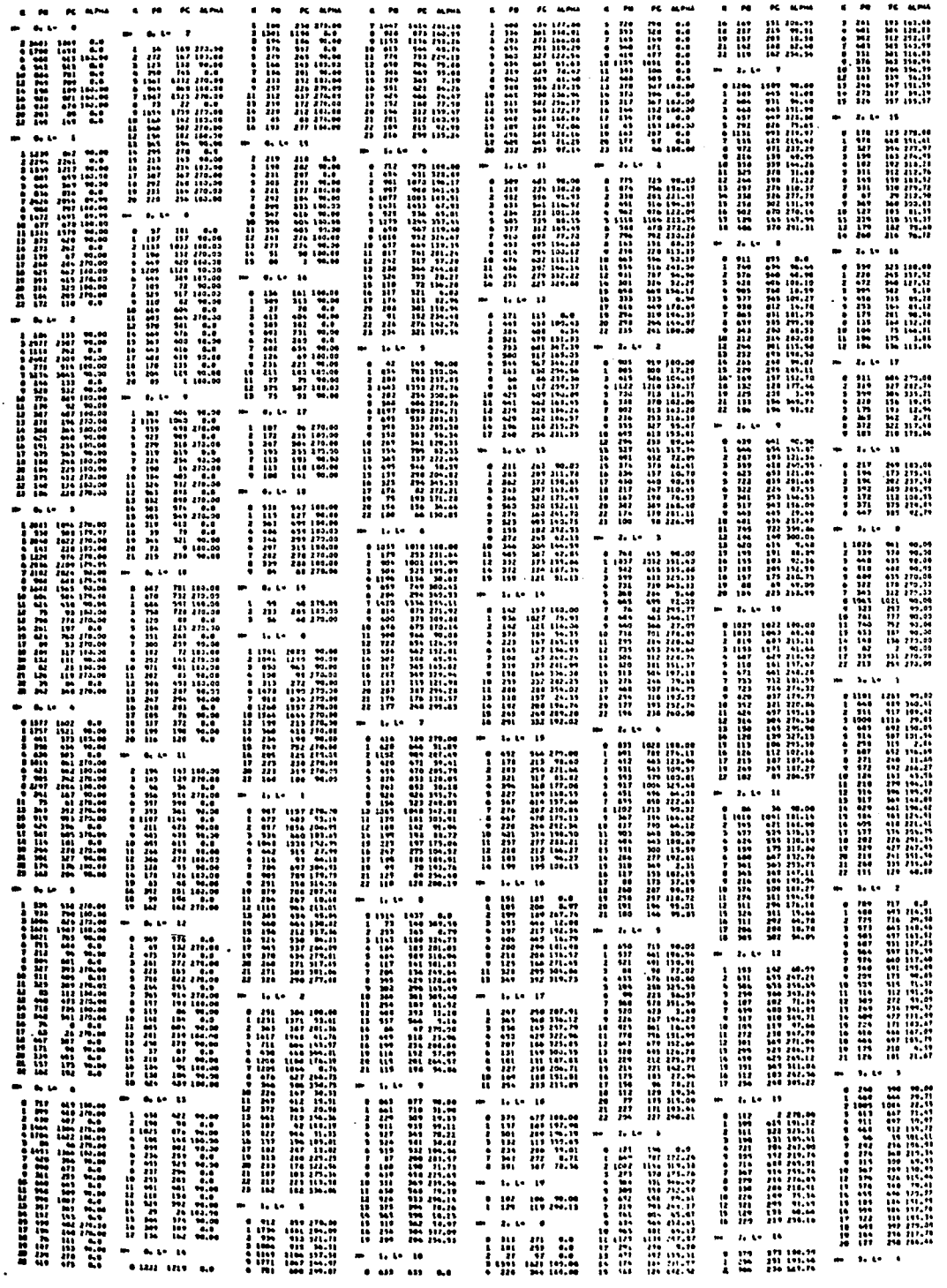

TABLE 4--Continued

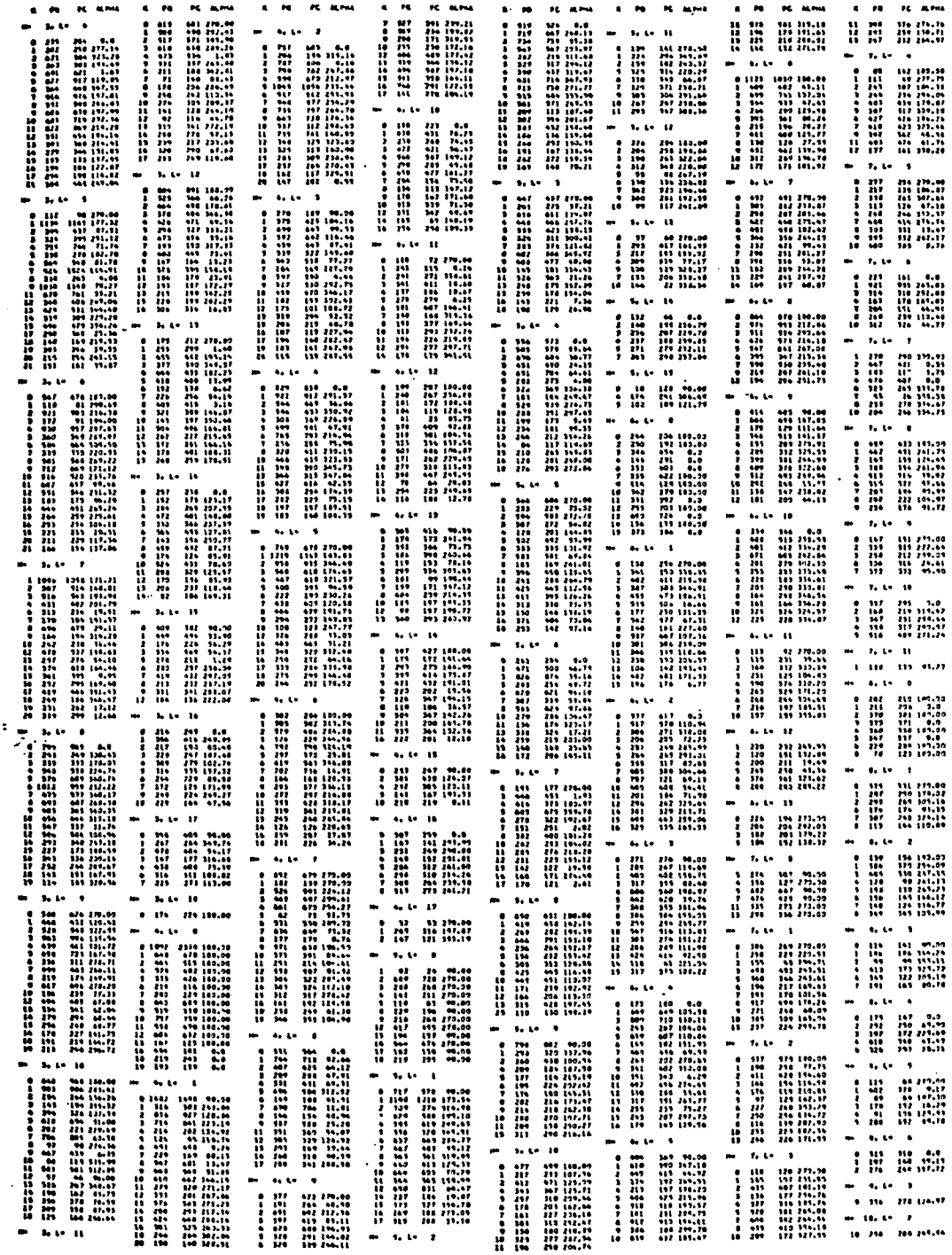

crystals were used to take the intensity data over a period of approximately 10 months. Several scale factors had to be applied to the data. For these reasons, the accuracy of the results for Cuglt are not what we would like. Therefore, differences that exist between the bond distances and bond angles of Cuglt and accepted values are due in part to the introduction of the errors discussed above. However, we were interested in configurational aspects of the structure and not necessarily small differences in bond angles and distances.

Discussion of the Structure

In Figure 2 is shown a projection of the structure onto the ac plane. The ether molecules are not shown in this projection. The numbering system of the peptide molecule and ether molecule is listed in Figure 1. The copper chelate of glycyl-l-leucyl-l-tyrosine, Cuglt, is a dimer consisting of two peptide molecules, A and B, two copper atoms, Cu(1) and Cu(2), and one water molecule, $H_2O(6)'$ shown in Figure 2. Peptide molecule A is chelated to Cu(1) through the terminal amino nitrogen atom N_1A and carbonyl oxygen O_1A from the glycyl residue. The peptide nitrogen, N_2A, and carbonyl oxygen, O_2A, of the leucyl residue are not involved in chelation to either of the two copper atoms. The second peptide nitrogen, N_3A, and carboxylic oxygen, O_3A, from the tyrosine residue are chelated to Cu(2).

Figure 2. ac Projection of Copper Complex of Glycyl-l-Leucy-l-Tyrosine. Ether molecule not shown in this projection.

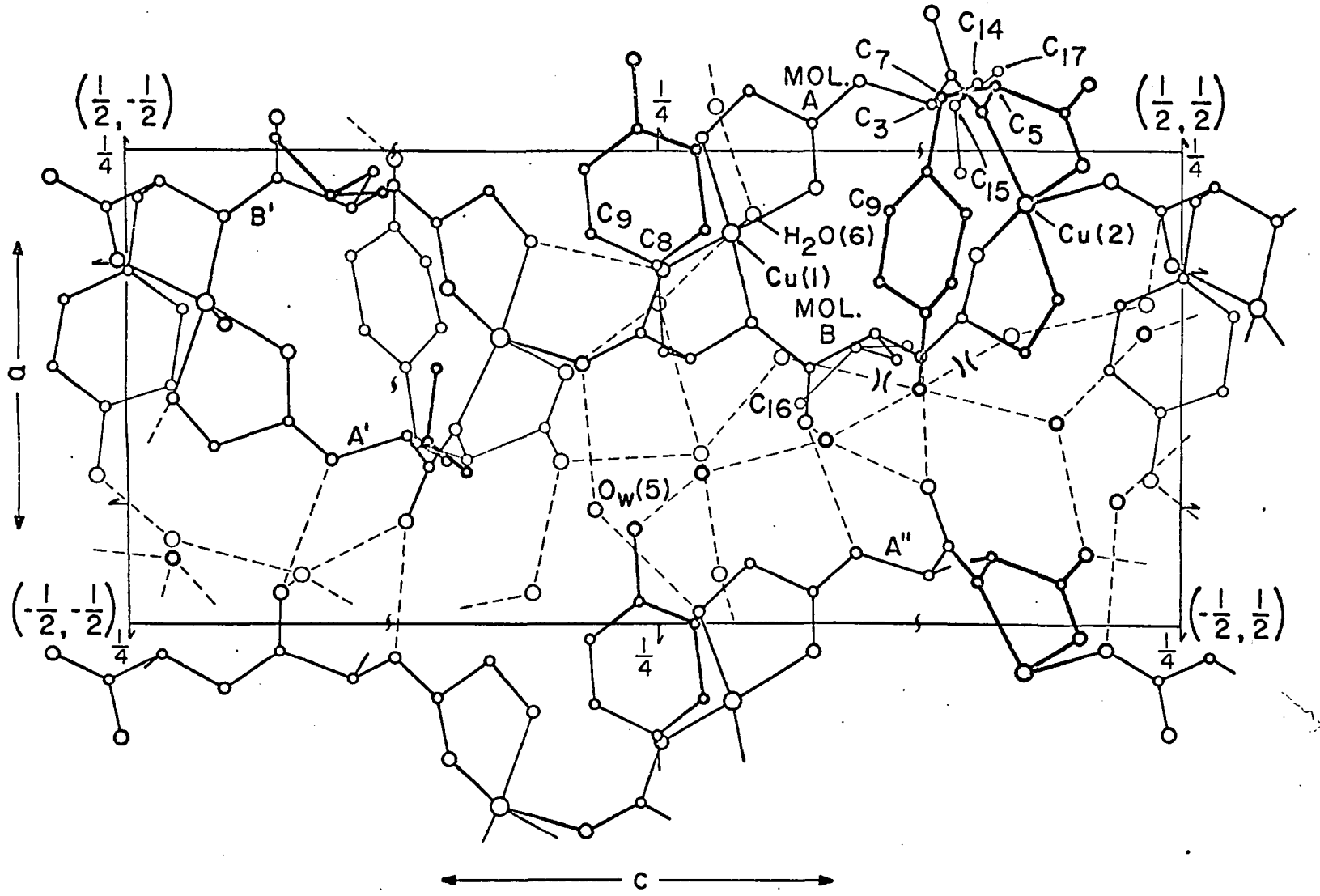

Phenolic carbon atoms C_7A, C_8A, and C_9A come in close proximity of the sixth position of Cu(2) (See Figure 6). Peptide molecule B is chelated to Cu(2) through the terminal amino nitrogen N_1B and carbonyl oxygen O_1B of the glycyl residue. As in molecule A and likewise for molecule B, the peptide nitrogen N_2B and carbonyl oxygen O_2B of the leucyl residue are not involved in chelation to either copper atom. Peptide nitrogen N_3B and carboxylic oxygen O_3B of the tyrosine residue are both chelated to Cu(1). The phenolic carbon atoms of molecule B, C_7B, C_8B, C_9B, and $C_{13}B$ are in close proximity of the sixth position of Cu(1) (See Figure 5). The close approach of the phenolic groups to the two copper ions is rather unusual and a discussion of this fact is given later. The dimers are formed by coordination of each of the peptide molecules to both copper atoms through their end groups; terminal amino nitrogens N_1 and carbonyl oxygens O_1 from the glycyl residues at one end and peptide nitrogens N_3 and carboxylic oxygens O_3 from the tyrosine residues at the opposite end. Peptide molecule B is further chelated to a symmetry related copper atom Cu(2)' through the carboxylic oxygen O_4B. Consequently, the carboxylic group of molecule B is shared by both copper atoms. This completes the coordination of Cu(2), and the coordination of Cu(1) is completed by a water molecule $H_2O(6)'$ at the fifth position. These observations illustrate that the two peptide molecules A and B are chelated in similar manner to the copper ions,

but the two peptide chains run in opposite directions. The dimers are united along the -c axis by the coordination bond between Cu(2)' and O_4B and also by a peptide-peptide hydrogen bond between O_3B and N_1B' of 2.91A°.

Peptide nitrogens N_2 and carbonyl oxygens O_2 of the leucyl residues that were not involved in chelation to either copper ion form N_2—H---O_2 hydrogen bonds to dimers related by a translation along the -a axis. Peptide nitrogen N_2B forms a hydrogen bond with O_2A'' of length 2.85A°, and carbonyl oxygen O_2B forms a hydrogen bond with N_2A'' of length 2.80A°. These two peptide-peptide hydrogen bonds are between peptide molecules extending in opposite directions. As a consequence of these two hydrogen bonds and the orientation of the two peptide units of each molecule which will be illustrated later, the structure of Cuglt is the anti-parallel chain pleated sheet configuration proposed by Pauling and Corey (13). The orientation of the two peptide units is best observed in Figure 3.

Figure 3 shows the bc projection of the structure. Two atoms, N_1 and C_1, of each molecule A and B were omitted from this projection. The twist or bend between peptide units occurs at C_3. Filling the cavity between dimers symmetry related along the b axis are water and ether molecules. The ether molecules are stacked as a column around the 2-fold screw axis parallel to a. The ether molecules lie very close to the bc plane, and no

Figure 3. bc Projection of Complex. Atoms N_1 and C_1 not shown in this projection. Molecules A and B are related to parameters in Table 3--by the operation ½-x, -y, ½+z.

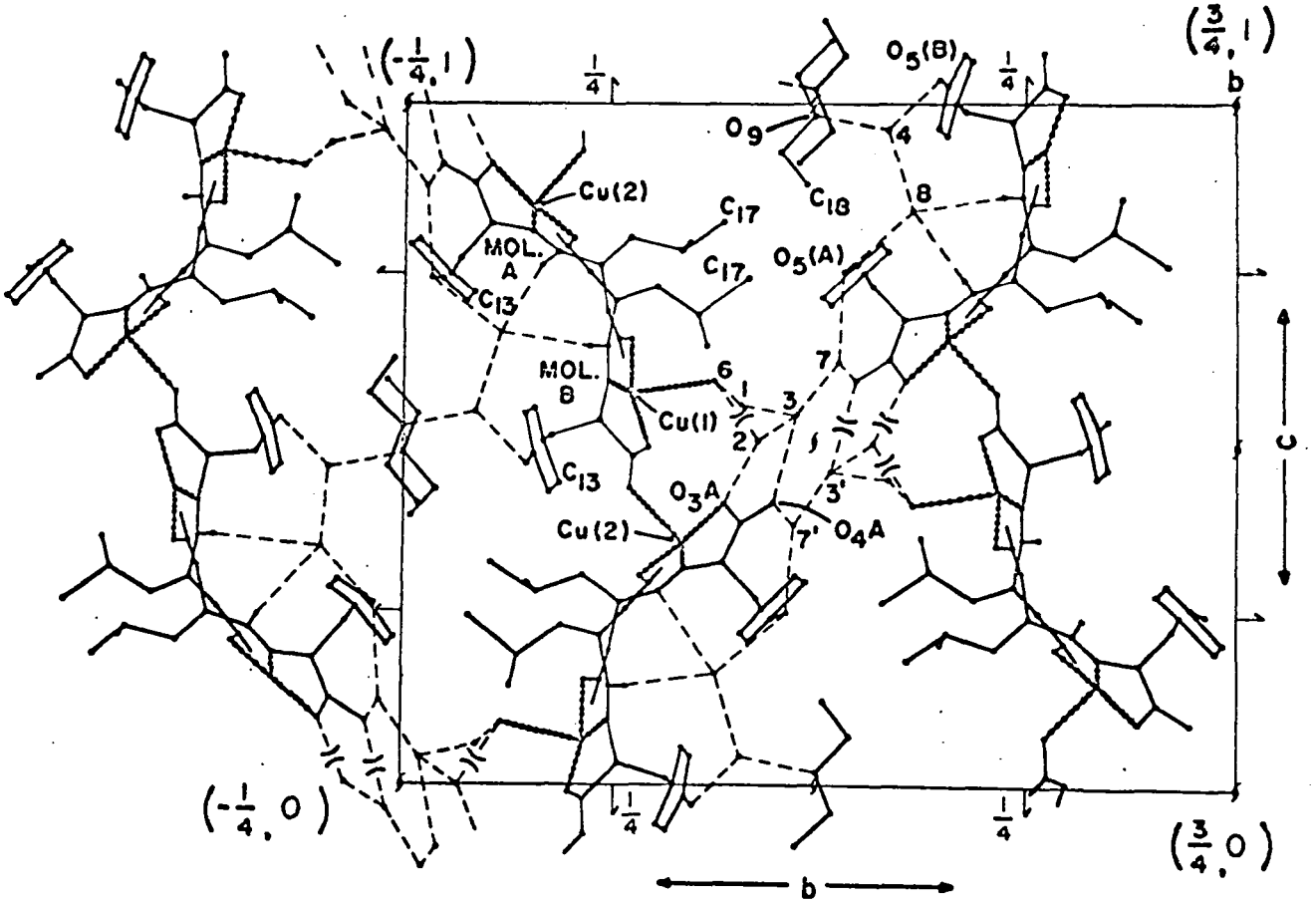

van der Waals' interactions exist between ether molecules as they are separated by ½a or approximately 4.6A°. The columns of ether are used to fill the hole that originates when the groups of similar polarity, isopropyl and phenolic groups locate themselves in the same general area. This is seen in Figure 3 if we consider the column of ether located at (-¼,½) in this projection. Therefore, ether is a necessary component of this structure for three reasons; (1) it was the size necessary to fill the hole, (2) of similar polarity of the phenolic and isopropyl groups, and (3) has available one oxygen for hydrogen bond formation to aid in its packing. The ether molecules themselves are packed by virtue of the hydrogen bond between ether oxygen O_9 and $H_2O(4)$ of length 2.90A°. Very weak van der Waals' interactions are observed between C_{18} of an ether molecule and C_7 and C_8 (3.60A° and 3.66A° respectively) of the phenolic group of molecule A. The role of the ether molecules in the crystal structure of the copper chelate of glycyl-l-leucyl-l-tyrosine is primarily space filling. The remaining cavity between dimers symmetry related is filled by water molecules that play an important part in packing.

Two hydrogen bond spirals are present in this structure. One of these spirals consists of two water molecules $H_2O(7)$ and $H_2O(3)$ and a peptide oxygen O_4A spiraling around a two-fold screw axis (¼,½). One

revolution of this hydrogen bond spiral can be traced in Figure 3 as $H_2O(7)$--2.75A°--$H_2O(3)$--2.87A°--O_4A--2.72A°--$H_2O(7)'$--2.75A°--$H_2O(3)'$--2.87A°--O_4A''--2.72A°--$H_2O(7)''$. O_4A'' and $H_2O(7)''$ are translated -a. This spiral is in turn united with the second hydrogen bond spiral consisting of water molecules only. The water molecules comprising the second spiral are $H_2O(6)$--2.55A°--$H_2O(1)$--3.23A°[1]--$H_2O(3)$--2.81A°--$H_2O(2)$--2.96A°--$H_2O(6)'$. $H_2O(6)'$ is translated -a. These two spirals fill the cavity between dimers in different layers and also pack peptide molecules symmetry related by the 2-fold axis at (¼,½) and those related by translation along the a axis. The packing role of the water molecules is observed with the direct participation of peptide oxygens O_4A and O_4A' in one of the hydrogen bond spirals. Furthermore, $H_2O(2)$, a part of the second spiral is hydrogen bonded to peptide oxygen O_3A of length 2.70A°, and $H_2O(6)$, a participant in the second spiral, is coordinated to Cu(1) and considered a part of the dimer. Further packing is furnished by $H_2O(1)$ with h-bond to N_1A' of length 3.09A° not shown in Figures 3 or 4. Additional water molecules aid in the packing of dimers by forming a hydrogen bond chain that includes atoms of the peptide molecules. The hydrogen bond chain extends between two columns of ether. Considering $H_2O(4)$ as the beginning of the chain it is

---

[1]See comment on page 71.

hydrogen bonded to the ether oxygen O_9 of length 2.90A°. This hydrogen bond has been mentioned previously. $H_2O(4)$ is further h-bonded to phenolic oxygen O_5B of length 2.45A°, and the chain continues with the h-bond from $H_2O(4)$ to $H_2O(8)$ of length 2.75A°. The two hydrogen bonds from $H_2O(8)$ to O_2B and O_2A' of length 3.06A° and 2.85A° pack dimers together along the a axis. The chain continues with the hydrogen bond from $H_2O(8)$ to O_5A of length 2.86A°. O_5A forms a h-bond with $H_2O(7)$ of length 2.93A° which constitutes the intersection of the hydrogen bond chain with the first h-bond spiral. The chain repeats itself on the opposite side of the spiral in the same manner as previously described up to the intersection with the h-bond spiral. The chain terminates at the column of ether located at (¼,0). The final water molecule that has not been considered is $H_2O(5)$. $H_2O(5)$ forms two hydrogen bonds shown in Figure 2 which are not a part of either of the two hydrogen bond spirals nor the hydrogen bond chain. $H_2O(5)$ forms a h-bond with O_4B of length 2.99A° and with N_1A'' of length 2.90A°.

Briefly summarizing the discussion, we have observed the chelate, Cuglt, to be a dimer. Each peptide molecule is coordinated to each copper ion in similar fashion. Both copper ions are five coordinated with a H_2O molecule and a carboxylic oxygen occupying the fifth position. The peptide molecules are in the anti-parallel

chain pleated sheet configuration with peptide-peptide hydrogen bonds formed by N_2 and O_2 of the leucyl residues which are not involved in chelation to copper. The ether molecule is used primarily to fill the hole created when groups of similar polarity, isopropyl and phenyl, locate themselves in the same general area. The water molecules have two roles, one of space filling and the other as packing. Two water molecules, $H_2O(8)$ and $H_2O(3)$, form four h-bonds; four water molecules, $H_2O(1)$, $H_2O(2)$, $H_2O(4)$, and $H_2O(7)$, form three h-bonds, and the remaining two water molecules, $H_2O(5)$ and $H_2O(6)$, form two hydrogen bonds each. In addition to the hydrogen bonds, $H_2O(6)$ form a coordination bond with Cu(1). Three peptide-peptide hydrogen bonds are observed in this structure. Table 5 summarizes the hydrogen bonding and van der Waals' interactions of less than $3.50A^{o}$.

The hydrogen bonds involving $H_2O(1)$ and $H_2O(1)'$ are probably inaccurate to a larger degree than other hydrogen bonds due to the disorder of this water molecule. The hydrogen bonds of $H_2O(1)'$ were not considered in the discussion because of the disorder, but we should point out that contacts of $H_2O(1)'$ with other atoms shown in Table 5 indicate a vacancy existed at this position in the structure. The hydrogen bonds formed by $H_2O(1)'$ were better than those formed by $H_2O(1)$.

Table 6 lists bond distances for the two peptide

TABLE 5

Intermolecular Bond Distances Less Than 3.50A°

Atom(1)	Atom(2)	Distance, A°	Formula		
A. Peptide-Peptide H-bonds					
N_2B	O_2A''	2.85	-1+x	y	z
O_2B	N_2A''	2.80	-1+x	y	z
O_3B	N_1B'	2.91	½-x	-y	-½+z
B. Peptide - H_2O H-bonds					
$H_2O(1)$*	N_1A	3.09	½+x	-y	½+z
$H_2O(2)$	O_3A	2.70	x	y	z
$H_2O(3)$	O_4A	2.87	x	y	z
$H_2O(4)$	O_5B	2.45	-½+x	½+y	1-z
$H_2O(5)$	O_4B'	2.99	½-x	-y	-½+z
$H_2O(5)$	N_1A''	2.90	-1+x	+y	z
$H_2O(7)$	O_4A	2.72	-½+x	½-y	1-z
$H_2O(7)$	O_5A'''	2.93	½+x	½-y	1-z
$H_2O(8)$	O_2B''	3.06	½+x	½-y	1-z
$H_2O(8)$	O_2A'''	2.85	-½+x	½-y	1-z
C. H_2O - H_2O H-bonds					
$H_2O(1)$*	$H_2O(3)$	3.23	x	y	z
$H_2O(1)$*	$H_2O(6)$	2.55	x	y	z
$H_2O(2)$	$H_2O(6)$	2.96	-1+x	y	z
$H_2O(2)$	$H_2O(3)$	2.81	x	y	z
$H_2O(3)$	$H_2O(7)$	2.75	x	y	z
$H_2O(4)$	$H_2O(8)$	2.75	x	y	z
D. Ether - H_2O Hydrogen bond					
O_9	$H_2O(4)$	2.90	x	y	z

TABLE 5--Continued

E. Hydrogen Bonds of $H_2O(1)'$*

Atom(1)	Atom(2)	Distance, A°	Formula		
$H_2O(1)'$	$H_2O(7)$	2.96	x	y	z
$H_2O(1)'$	$H_2O(5)$	2.98	-x	½+y	½-z
$H_2O(1)'$	N_1A	2.87	1-x	½+y	½-z

F. van der Waals' Interactions of Less Than 3.50A°

Interaction		Form.@	Dist., A°	Interaction		Form.@	Dist., A°
C_1A	O_2B	(2)	3.16	O_5B	O_w5	(6)	3.39
C_2A	O_2B	(2)	3.43	C_1A	O_w5	(6)	3.23
C_1B	O_2A	(2)	3.17	N_1B	O_w1'*	(5)	3.25
C_2B	O_2A	(2)	3.45	C_1B	O_w1*	(2)	3.34
O_2A	O_2B	(2)	3.20	$C_{11}B$	O_w4	(4)	3.34
$C_{17}A$	O_5A	(3)	3.48	$C_{12}B$	O_w4	(4)	3.33
O_4A	O_w1'*	(4)	3.26	N_3A	O_w5	(7)	3.50
$C_{11}A$	O_w7	(5)	3.48	O_w1'*	O_w6	(5)	3.31
$C_{10}A$	O_w8	(5)	3.45	O_w7	O_w2	(1)	3.46
$C_{15}B$	O_w6	(2)	3.19				
C_7B	O_w4	(4)	3.49				
N_1B	O_w2	(1)	3.50				

*$H_2O(1)$ - Disordered Water (2/3)

$H_2O(1)'$- Disordered Water (1/3)

@

(1)	x	y	z
(2)	-1+x	y	z
(3)	-x	-½+y	½-z
(4)	½+x	½-y	1-z
(5)	-½+x	½-y	1-z
(6)	1+x	y	z
(7)	½-x	-y	½+z

TABLE 6

Bond Distances

Bond	Mol.A	Mol.B	Av. Bond Distances Molecules A and B	Freeman(2)
N_1-C_1	1.44(3)	1.47(3)	1.46(3)	1.48(007)
C_1-C_2	1.47(3)	1.56(3)	1.51(3)	1.53(006)
C_2-O_1	1.27(2)	1.26(2)	1.27(2)	1.26(007)
C_2-N_2	1.30(2)	1.25(2)	1.28(2)	1.30(004)
N_2-C_3	1.54(2)	1.52(2)	1.53(2)	1.45(006)
C_3-C_4	1.50(3)	1.53(3)	1.52(3)	1.53(006)
C_4-O_2	1.26(2)	1.28(2)	1.27(2)	1.26(007)
C_4-N_3	1.29(2)	1.33(3)	1.31(3)	1.30(004)
N_3-C_5	1.42(3)	1.47(3)	1.45(3)	1.45(006)
C_5-C_6	1.57(3)	1.53(3)	1.55(3)	1.52(005)
C_6-O_3	1.24(3)	1.29(2)	1.27(3)	1.28(007)
C_6-O_4	1.29(3)	1.25(2)	1.27(3)	1.23(005)

Phenolic Group

Bond	Molecule A	Molecule B	Average
C_5-C_7	1.62(3)	1.50(3)	1.56(3)
C_7-C_8	1.52(4)	1.60(4)	1.56(3)
C_8-C_9	1.30(4)	1.43(4)	1.37(4)
C_9-C_{10}	1.44(4)	1.39(4)	1.42(4)
C_{10}-C_{11}	1.44(4)	1.25(4)	1.35(4)
C_{11}-C_{12}	1.25(4)	1.36(4)	1.30(4)
C_{12}-C_{13}	1.33(4)	1.53(4)	1.43(4)
C_{13}-C_8	1.48(4)	1.26(4)	1.37(4)
C_{11}-O_5	1.43(4)	1.39(4)	1.41(4)

TABLE 6--Continued

Isopropyl Group			
Bond	Molecule A	Molecule B	Average
C_3-C_{14}	1.53(3)	1.56(3)	1.55(3)
C_{14}-C_{15}	1.56(3)	1.53(4)	1.55(4)
C_{15}-C_{16}	1.52(4)	1.56(5)	1.54(5)
C_{15}-C_{17}	1.53(4)	1.71(5)	1.62(5)
Ether Molecule			
C_{18}-C_{19}	1.38(8)		
C_{19}-O_{20}	1.42(7)		
O_{20}-C_{21}	1.26(6)		
C_{21}-C_{22}	1.40(8)		

molecules A and B. Figure 4 shows the bond distances within the peptide backbone for molecules A and B. Bond angles are shown in Table 7. The bond distances are fairly consistent within the peptide backbone. The average bond distances of molecules A and B shown in column 4 compare favorably with those of copper complexes of amino acids and peptides summarized by Freeman (2) and listed in column 5. The largest deviation occurring was 0.08A° for the N_2-C_3 bond.

The bond distances of the phenyl group, isopropyl group, and the ether molecule are also listed in Table 6. The average values of the bond distances within the isopropyl group and phenyl group of molecules A and B are shown in column 4. Deviations from a normal C-C bond distance of 1.54A° or a normal aromatic C-C bond distance of 1.40A° can be attributed to inaccuracies in the structure determination. The standard deviations of the bond lengths of the isopropyl groups, phenolic groups, and the ether molecules are larger than the standard deviations of the bond lengths within the peptide backbone. This conceivably is due to the larger temperature movement of the atoms involved.

The configuration around both copper atoms, Cu(1) and Cu(2) are shown in Figures 5 and 6 respectively and listed in Table 8. Column 4 of Table 8 lists the average bond distances between copper and ligand atoms comprising

Figure 4. Intramolecular Bond Distances of the Peptide Backbone of Molecules A and B.

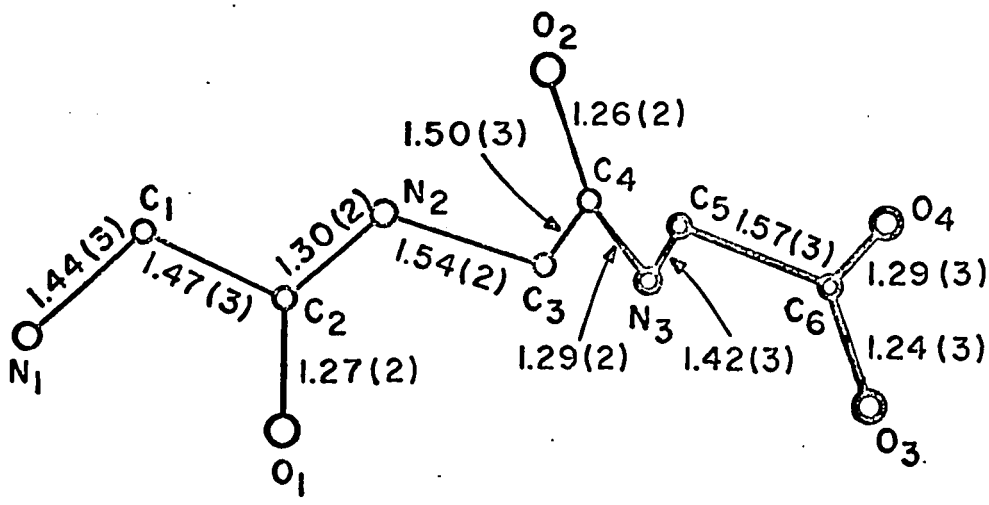

MOL. A

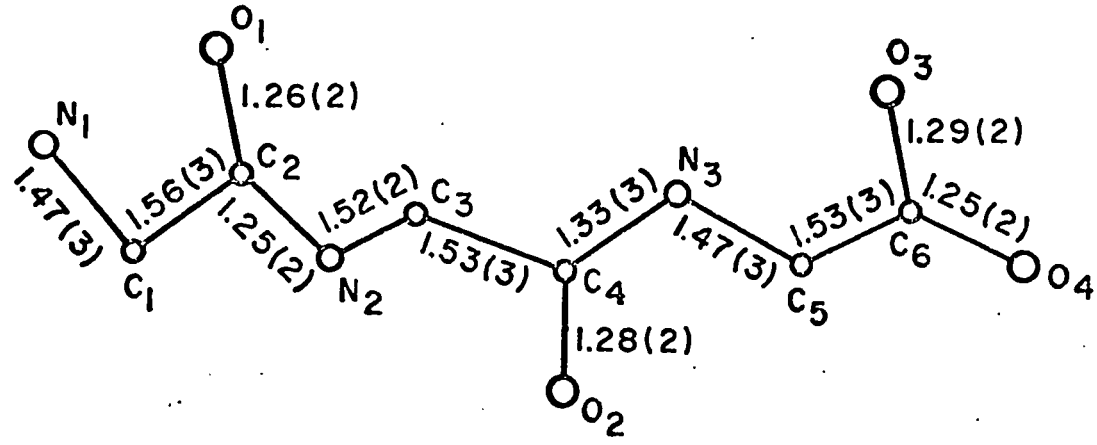

MOL. B

TABLE 7
Bond Angles

Angle	Mol.A, °	Mol.B, °
$N_1C_1C_2$	110(2)	109(2)
$C_1C_2O_1$	120(2)	118(2)
$C_1C_2N_2$	117(2)	117(2)
$O_1C_2N_2$	123(2)	125(2)
$C_2N_2C_3$	123(2)	123(2)
$N_2C_3C_4$	105(2)	106(1)
$N_2C_3C_{14}$	109(2)	103(1)
$C_{14}C_3C_4$	112(2)	112(2)
$C_3C_4O_2$	121(2)	119(2)
$C_3C_4N_3$	117(2)	117(2)
$O_2C_4N_3$	122(2)	124(2)
$C_4N_3C_5$	115(2)	114(2)
$N_3C_5C_6$	107(2)	105(2)
$N_3C_5C_7$	115(2)	114(2)
$C_6C_5C_7$	108(2)	112(2)
$C_5C_6O_3$	119(2)	119(2)
$C_5C_6O_4$	115(2)	118(2)
$O_3C_6O_4$	126(2)	121(2)
$C_5C_7C_8$	110(2)	112(2)
$C_7C_8C_9$	125(2)	117(2)
$C_7C_8C_{13}$	118(2)	120(2)
$C_9C_8C_{13}$	116(3)	122(3)
$C_8C_9C_{10}$	124(2)	114(3)

TABLE 7--Continued

Angle	Mol.A, °	Mol.B, °
$C_9C_{10}C_{11}$	113(2)	127(3)
$C_{10}C_{11}C_{12}$	121(3)	122(3)
$C_{10}C_{11}O_5$	111(2)	125(3)
$C_{12}C_{11}O_5$	126(3)	113(2)
$C_{11}C_{12}C_{13}$	123(3)	114(2)
$C_8C_{13}C_{12}$	118(3)	121(2)
Isopropyl Group		
$C_3C_{14}C_{15}$	115(2)	112(2)
$C_{14}C_{15}C_{16}$	106(2)	112(3)
$C_{14}C_{15}C_{17}$	108(2)	105(2)
$C_{16}C_{15}C_{17}$	111(2)	106(3)
Ether Molecule		
$C_{18}C_{19}O_9$	107(4)	
$C_{19}O_9C_{20}$	115(4)	
$O_9C_{20}C_{21}$	118(5)	

Figure 5. Coordination Sphere of Cu(1) in $Cu_2(glt)_2 \cdot 8H_2O \cdot Et_2O$

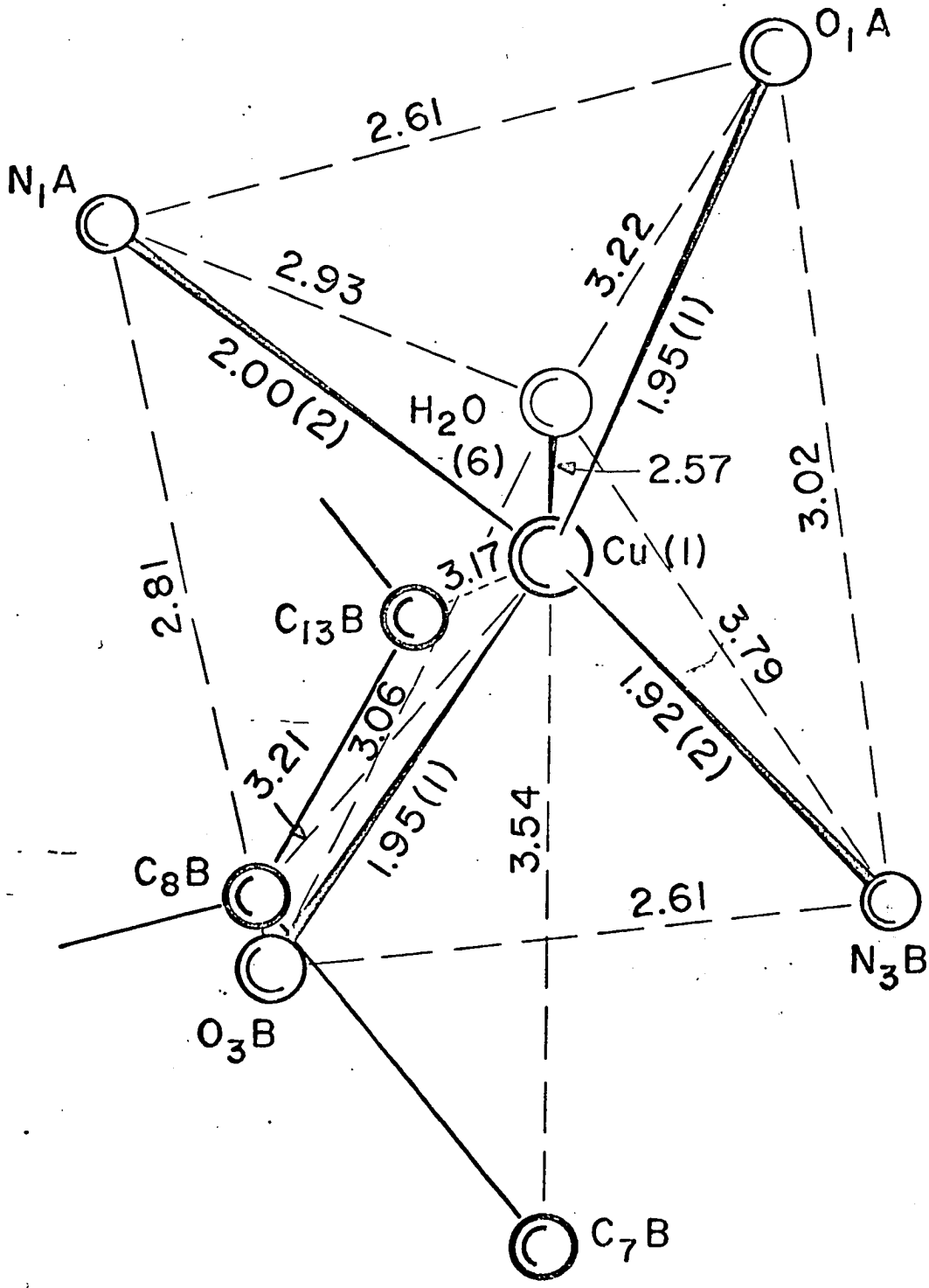

Figure 6. Coordination Sphere of Cu(2) in $Cu_2(glt)_2 \cdot 8H_2O \cdot Et_2O$

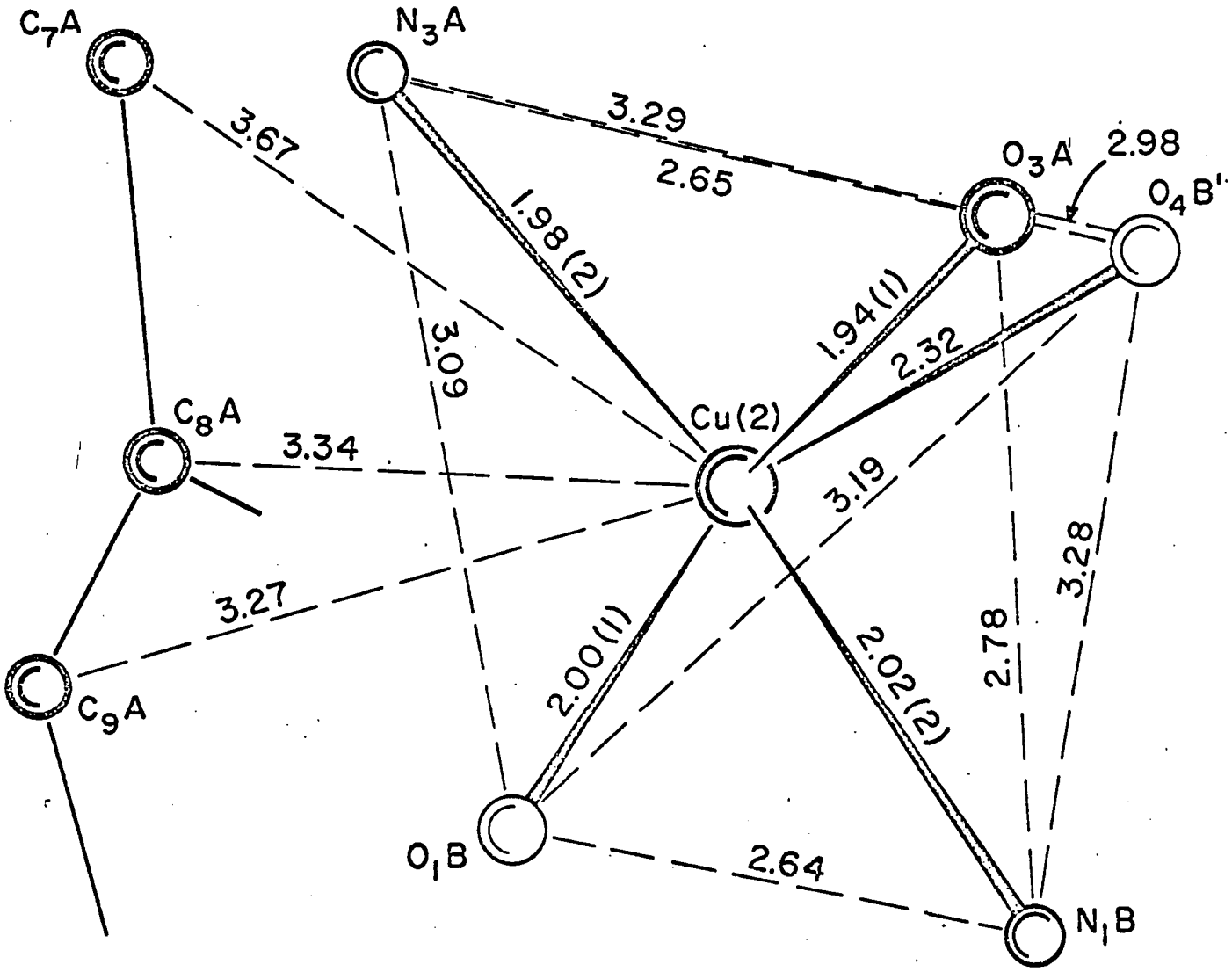

TABLE 8

Coordination Around Copper Ions

Bond Distances			
Bond	Cu(1), A^{o}	Cu(2), A^{o}	Freeman(2)
Cu-N_1	2.00(2)	2.02(2)	2.01
Cu-O_1	1.95(1)	2.00(1)	1.96
Cu-N_3	1.92(2)	1.98(2)	1.92
Cu-O_3	1.95(1)	1.94(1)	1.97
Cu-O	2.57(2)	2.32(2)	

Bond Angles		
Angle	Cu(1), Degrees	Cu(2), Degrees
O_3 Cu N_3	84.9(6)	85.2(7)
N_1 Cu N_3	165.6(8)	161.2(7)
O_1 Cu N_3	102.5(6)	102.3(6)
O_3 Cu N_1	90.8(8)	89.1(7)
O_3 Cu O_1	171.8(6)	171.0(6)
N_1 Cu O_1	82.7(7)	82.3(6)
Cu N_1 C_1	112(1)	113(1)
Cu O_1 C_2	115(1)	116(1)
Cu O_3 C_6	111(1)	113(2)
Cu N_3 C_5	109(1)	109(1)

TABLE 8--Continued

Least Squares Planes	

A. Coordination sphere of Cu(1)

Plane 1. N_1A, O_1A, O_3B, N_3B

$1.48x + 23.89y - 7.14z = -.63$

Atom	Dist. from L.S. Plane(A^o)
N_1A	+ .16
O_1A	- .15
O_3B	- .16
N_3B	+ .15
Cu(1)	- .08
$H_2O(6)$	-2.52

Plane 2. N_1A, O_1A, N_3B, O_3B, Cu(1)

$1.48x + 23.90y - 7.13z = -.65$

N_1A	.17
O_1A	- .13
O_3B	- .14
N_3B	+ .16
Cu(1)	- .06
$H_2O(6)$	-2.50

B. Coordination sphere of Cu(2)

Plane 3. N_1B, O_1B, O_3A, N_3A

$1.73x - 18.41y + 14.19z = 3.79$

N_1B	- .13
O_1B	+ .12
O_3A	+ .13
N_3A	- .12
Cu(2)	+ .19
O_4B'	+2.50

TABLE 8--Continued

Plane 4. N_1B, O_1B, O_3A, N_3A, Cu(2)

$$1.72x - 18.39y + 14.22z = 3.83$$

Atom	Dist. from L.S. Plane(A^o)
N_1B	- .16
O_1B	+ .08
O_3A	+ .09
N_3A	- .16
Cu(2)	+ .15
O_4B'	+2.46

the coordination sphere for various copper complexes of amino acids and peptides (2) for comparison with those of Cu(1) and Cu(2). The water molecule $H_2O(6)$ occupies the fifth position of Cu(1) at a distance of 2.57A° whereas the fifth position around Cu(2) is occupied by a carboxylic oxygen O_3B' at a distance of 2.32A°. Least squares plane 1 was calculated with atoms N_1A, O_1A, O_3B, and N_3B. The average deviation of the atoms from this plane was 0.16A°. Cu(1) deviated 0.08A° from this plane. Plane 2 was calculated using the four ligands atoms and Cu(1). The average deviation of the ligand atoms was 0.16A°. Cu(1) deviated 0.06A° from this plane. Plane 3 was calculated with the four closest ligand atoms of Cu(2), N_1B, O_1B, O_3A, and N_3A. The average deviation of these atoms from plane 3 was 0.13A°. Cu(2) deviated 0.19A° from this plane. Plane 4 was calculated with Cu(2) and its four closest ligands atoms. The average deviation of the four closest ligand atoms of Cu(2) from plane 4 was 0.12A°. Cu(2) deviated 0.15A° from plane 4. The average deviations of the ligand atoms around Cu(1) (0.16A°) was slightly larger than the deviation of the ligand atoms around Cu(2) (0.13A°). However, this data indicate the four ligand atoms do not form a very good plane around the copper ions. The stronger interaction between Cu(2) and O_4B' displaces Cu(2) from the best least squares planes 3 and 4 of .19A° and .15A° respectively, whereas the weaker interaction between Cu(1)

and $H_2O(6)$ displaces Cu(1) by approximately one-half this amount, or .08A° and .06A° from L.S. planes 1 and 2 respectively. Both copper atoms Cu(1) and Cu(2) are displaced toward the ligand atom occupying the fifth position. Furthermore, both copper atoms are at all times displaced in the same direction as the oxygen atoms whereas in all instances the nitrogen atoms are displaced in the opposite direction. The length of the sides completing the square pyramids in Figures 5 and 6 are in close agreement. The largest distance occurs for the interaction between the carbonyl oxygens O_1 and peptide nitrogens N_3 of 3.02A° for Cu(1) and 3.09A° for Cu(2). Water molecule $H_2O(6)$ is not equidistant from the four ligand atoms of Cu(1), shown in Figure 5. This molecule is 2.93A° from N_1A which is the closest approach and 3.79A° from N_3B which is the longest distance. Carboxylic oxygen O_4B' assumes a position quite near the perpendicular axis of the least squares plane of Cu(2) shown in Figure 6. This atom is furthest removed from N_3A of length 3.29A° and closest to O_3A of length 2.98A°. The sixth position around both copper atoms is unoccupied. However, the hole created by this vacancy is filled by atoms from the phenolic groups. Phenolic carbon atoms C_8B and $C_{13}B$ are at distances of 3.21A° and 3.17A° respectively from Cu(1). Phenolic carbon atoms C_8A and C_9A are at distances of 3.34A° and 3.27A° respectively from Cu(2).

At this position around Cu(1) phenolic carbon atoms C_8B, $C_{13}B$, and C_7B are at distances of 3.34A, 3.17A, and 3.54A respectively. $C_{13}B$, which interacts strongest, is located near the 6th position of Cu(1). Phenolic carbon atoms C_7A, C_8A, and C_9A are at distances of 3.67A, 3.34A, and 3.27A respectively form Cu(2). The strongest interaction, Cu(2)----C_9A(3.27A), is located nearest the 6th position. One example of a similar type of interaction is given in the literature. In the structure of bis-(N-phenylsalicylaldimato) copper (II) (20) a distance of 3.45A is reported between the copper ion and a carbon atom of one of the benzene rings. The copper ion is four coordinated and located on a center of symmetry. The carbon atom is near the 6th coordination position. These three examples of strong interactions (especially for molecules A and B) between aromatic rings and copper ions suggest that these are π-interactions.

Least squares planes through various atoms of the peptide backbone are listed in Table 9. The carboxyl group of each molecule, A and B, comprising atoms C_5, C_6, O_3, and O_4 are planar. The largest deviation was -.06 for carbon atom C_6A. Both peptide nitrogens N_3A and N_3B are rotated 0.37A° and -.39A° respectively out of the plane of the carboxylic groups. A similar rotation of the nitrogen out of the plane of the carboxylic group occurred for bis(l-serinato) Cu(II), and this rotation seemed to be consistent with formation of a chelate for both amino acids and peptides.

TABLE 9

Least Squares Planes for Peptide Backbone

The equations of the planes are expressed in the form

$Ax + By + Cz = D$

where D is the origin to plane distance.

A. Carboxyl Groups

C_5, C_6, O_4, O_3

Atom	Dev.Mol.A	Dev.Mol.B	A	B	C	D
				(Mol.A)		
C_5	-.008	.02	5.02	-17.12	10.90	4.33
C_6	.03	-.06				
O_4	-.01	.02		(Mol.B)		
O_3	-.01	.02	4.93	+19.24	-8.48	.28
N_3	.37	-.39				
Cu@	-.09(2)	.18(1)				

B. Glycyl-leucyl Peptide Unit

Plane 1. C_1, C_2, O_1, N_2, C_3

				(Mol.A)		
C_1	+.04	-.02	.32	-24.86	5.48	1.32
C_2	-.02	+.02				
O_1	-.007	-.03		(Mol.B)		
N_2	-.06	.02	1.16	19.29	-13.70	-2.90
C_3	+.04	-.02				
N_1	+.07	.08				
Cu@	-.11(1)	.31(2)				

Plane 2. C_1, C_2, O_1, N_2

				(Mol.A)		
C_1	-.001	-.005	.37	-24.57	6.27	1.45
C_2	-.004	.02				
O_1	.002	-.006		(Mol.B)		
N_2	.002	-.006	1.18	19.56	-13.44	-2.80
N_1	-.012	.12				
Cu@	-.18(1)	.34(2)				
C_3	.16	-.07				

TABLE 9--Continued

C. Leucyl-Tyrosine Peptide Unit

Plane 3. C_3, C_4, O_2, N_3, C_5

Atom	Dev. Mol.A	Dev. Mol.B	A	B	C	D
				(Mol.A)		
C_3	- .02	-.02	2.89	-9.69	18.37	6.43
C_4	- .002	.02				
O_2	- .008	-.05		(Mol.B)		
N_3	- .03	.008				
C_5	- .02	-.01	2.78	24.40	2.50	.56
N_2	-1.01	.91				
Cu[@]	.27(2)	-.16(1)				

Plane 4. C_3, C_4, O_2, N_3

				(Mol.A)		
C_3	.001	-.006	2.91	-10.14	18.20	6.37
C_4	- .005	.020				
O_2	.002	-.008		(Mol.B)		
N_3	.002	-.008	2.77	24.37	2.72	.59
N_2	- .980	.930				
C_5	- .080	-.040				
Cu[@]	.23(2)	-.180(1)				

[@]The number in parenthesis refer to the copper ion.

The copper ions are displaced from the plane of the carboxyl groups. Planes through the peptide units show a remarkable deviation from planarity. In Plane 1 of the glycyl-leucyl peptide unit, the nitrogen atom N_2A is displaced .06A°. Carbon C_3A deviated .16A° from Plane 2, but with it included in the calculation a deviation of only .04A° occurred. However, these deviations from planarity are probably attributed to inaccuracies of the structure determination. One further observation is that neither copper ion was in the planes of the two peptide units. One of the more interesting features of this structure was the configuration of the peptide molecules themselves which we shall describe next.

The configuration of the peptide backbone can be described by considering the rotation around specific bonds. At the 1965 Gordon conference on Proteins, conventions and nomenclature (21) were proposed for describing the configuration of peptides, polypeptides, and proteins. The nomenclature as applied to glycyl-l-leucyl-l-tyrosine is shown in Figure 7. The angles ϕ_i , Ψ_i , and ω_i are positive for a right-handed rotation. When looking along any bond, in the direction from terminal nitrogen to the carboxyl group, the far end rotates clockwise relative to the near end. The conformation representing the fully stretched polypeptide chain characterized by the rotational angles $\phi_i = \Psi_i = \omega_i = 0$ is the standard conformation.

Figure 7. Standard Rotational Angles (Edsall, et al. 1966) as Applied to Glycyl-l-Leucyl-l-Tyrosine.

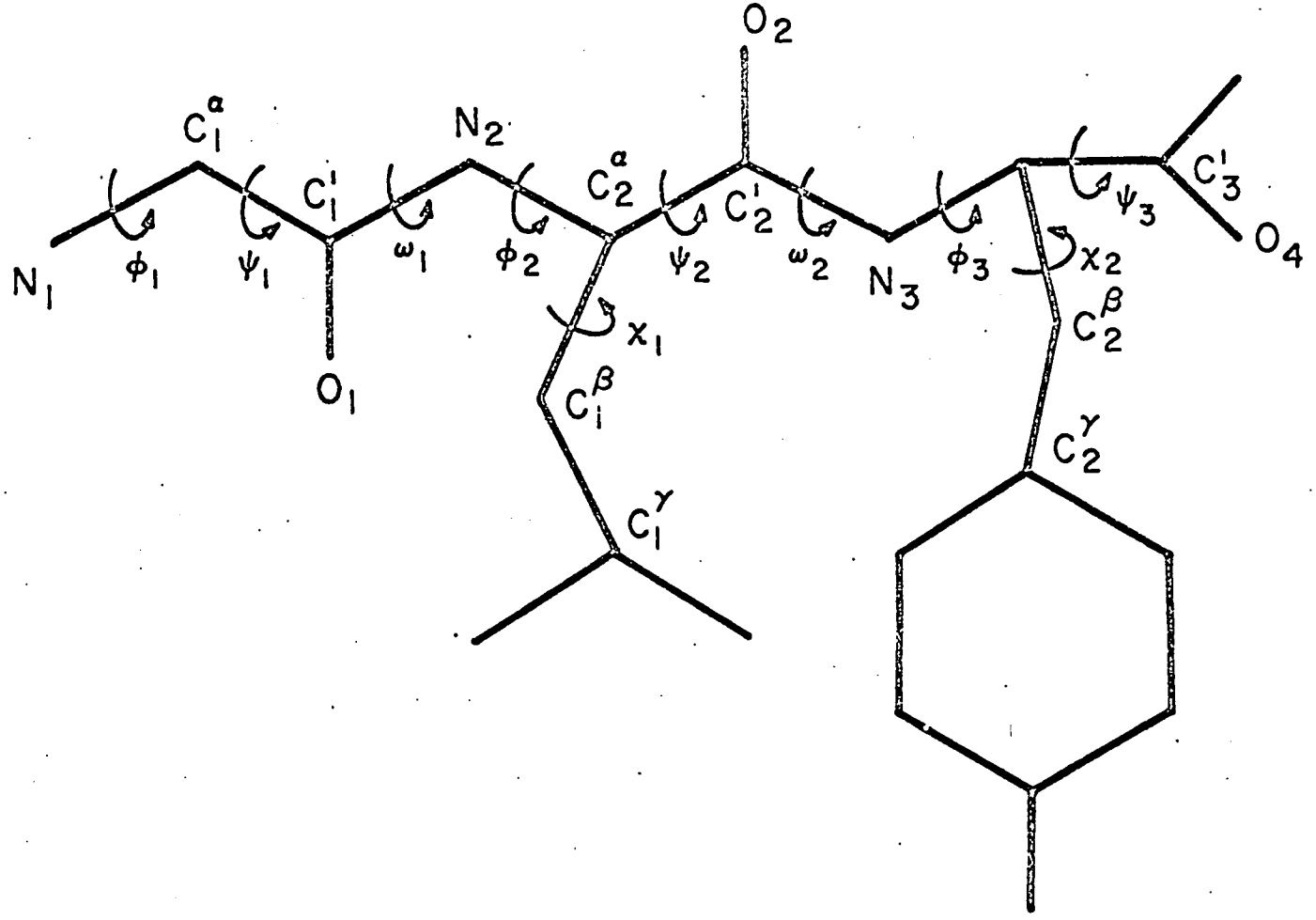

This conformation can be described by the following relationships (See Figure 7): C^{α}-C' bond cis to N-H bond with respect to rotation around the N-C^{α} bond (ϕ); N-C^{α} bond cis to C'-O bond with respect to rotation around the C^{α}-C' bond (Ψ); trans conformation of the peptide bond, i.e., C'-O bond trans to N-H bond (ω). Rotational angles ϕ_i, Ψ_i, and ω_i were determined by calculating the angle between the respective planes. The sense of rotation for the side chains is right handed about any bond. Looking in the direction of numbering, the sense is taken to be positive (as in the definition of rotation for the backbone). The planar eclipsed (cis) conformation is the choice of the zero angle denoted by $\chi_j = 0$. For the C^{α} C^{β} bond, the N-C^{α} and the C^{β}- C^{γ} bonds are used to define χ_1. The standard conformation denoting $\chi_j = 0$ has the C^{β} - C^{γ} bond cis or eclipsed with the N-C^{α} bond. This same conformation is used as we proceed down the chain. The rotational angles of Cuglt are listed in Table 10.

Due to steric hindrances between atoms comprising adjacent peptide units, only certain values of the rotational angles ϕ_i and Ψ_i are allowed. Using certain criteria of minimum contact distances between various atoms of the peptide units, Ramakrisman and Ramachandran (15) have worked out conformational maps for various types of peptides and for three values of the angle N-C^{α} - C'(τ). The conformational map computed with the presence of a C^{γ}

TABLE 10

Rotational Angles of Cu_2(gly-l-leu-l-tyr)$_2$ $8H_2O \cdot Et_2O$

Angle	Mol.A, Degrees	Mol.B, Degrees
ϕ_1	4.7	2.4
Ψ_1	1.1	3.7
ω_1	7.2	3.5
ϕ_2	129.9	131.4
Ψ_2	220.7	218.7
ω_2	3.0	3.0
ϕ_3	148.9	141.8
Ψ_3	19.6	23.1
χ_1	307.0	176.1
χ_2	54.4	58.7

carbon atom can be applied to glt. The values of χ used in their computations were $\chi = 60^{\circ}$, left skew, $\chi = 180^{\circ}$, trans, and $\chi = 300^{\circ}$, right skew. The conformational map for this case with $\tau = 110^{\circ}$ is shown in Figure 8. This conformational map has three different allowed areas. The area in the upper left hand corner represents the pleated sheet configuration. The areas labeled α_L and α_R are for the left hand alpha helix and right hand alpha helix respectively. The values of ϕ_2 and Ψ_2 for molecules A and B (See Table 10) were plotted in Figure 11 represented by $\otimes$, and the value of τ was 105° and 106° for molecules A and B respectively. Their values fall on the extreme outer limits of the allowed regions. However, the accuracy of the structure determination limits the significance of the close approach of these values to the "unallowed" regions.

The values of $306^{\circ}48'$ and $180^{\circ}0'$ for χ_1, A and B respectively, show that C_1^{γ} of the isopropyl groups occupies two of the three positions usually found for this atom. C_1^{γ} of molecule B is in the trans position, and C_1^{γ} of molecule A is in the right skew position. The χ_2 values of $54^{\circ}3'$ and $58^{\circ}3'$ for A and B respectively illustrate that the two C_2^{γ} carbon atoms of the phenyl groups are both in the left skew position. Ramachandran and Lakshminarayn (22) state that the phenyl group in other known structures occupied the trans position for five

Figure 8. Conformational Map Ramakrisman and Ramachandran (15). Allowed regions for C alone_____, (1) --------C in left skew position, 60, (2) C in trans position....., and (3) C in right skew position -.-.-.-. The position on molecules A and B is plotted as

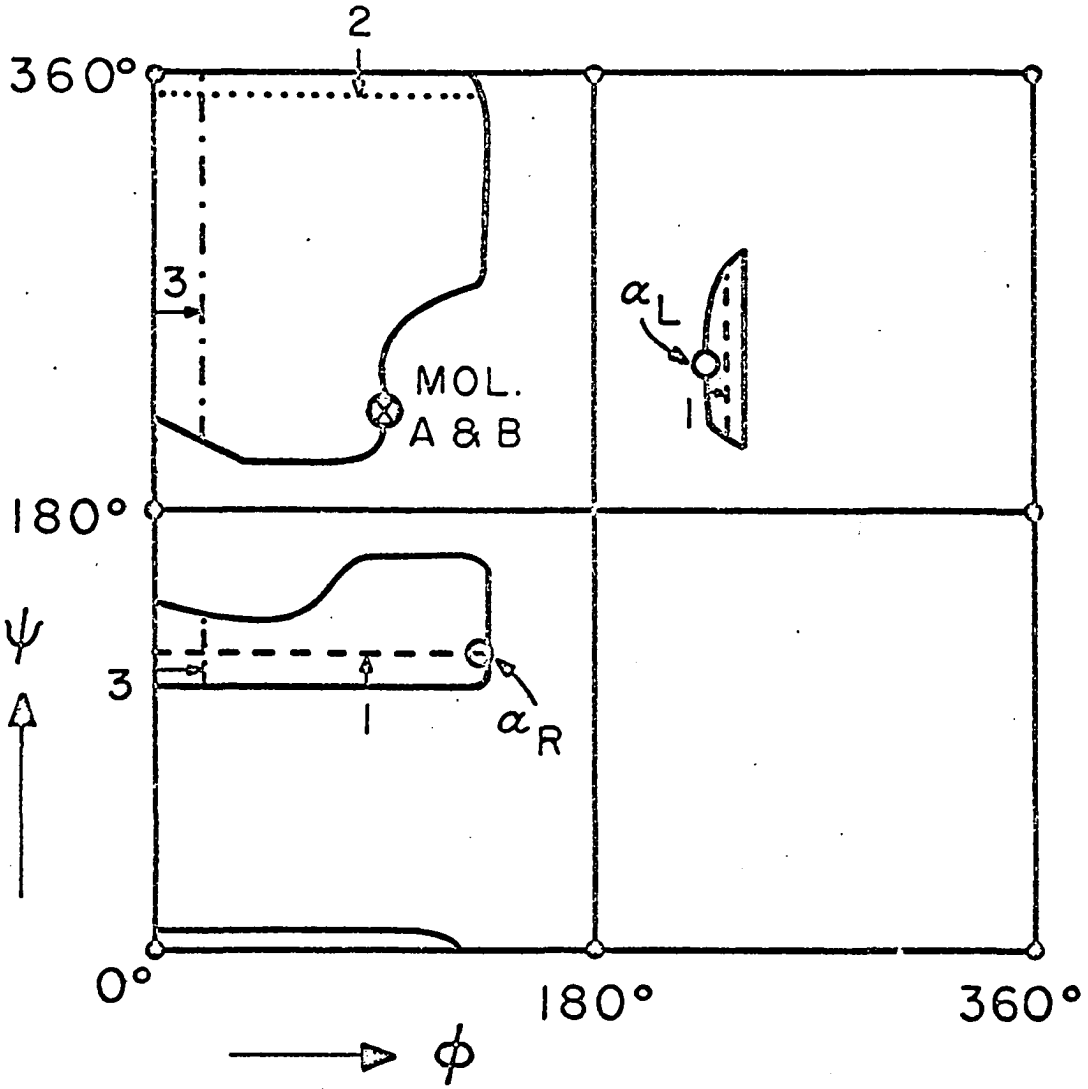

structures.

The rotational angles ϕ_1 and Ψ_1 and ϕ_3 and Ψ_3 cannot be used as plots in the conformational maps. The criteria being rotational angles between two adjacent peptide units which ϕ_3 and Ψ_3 are not. However, the values of Ψ_3 of $19^{\circ}14'$ and $23^{\circ}12'$ for A and B respectively, illustrate that the peptide nitrogens of the tyrosine residue are rotated out of the plane of the carboxyl group. The similarity of the rotational angles of A and B illustrate that the peptide molecules themselves are in the same configuration. The rotational angles ϕ_2 compare favorably with a value of 117.8° proposed by Pauling and Cory (13) for the pleated sheet configuration. Moreover, the configuration of Cuglt conforms to the anti-parallel pleated sheet configuration proposed by Pauling and Corey (13). The pleated sheet configuration has the C^{α} - H bond trans to both N-H and C'-O which is observed for both molecules A and B. The anti-parallel pleated sheet configuration consists of two chains running in opposite directions. This too is observed for Cuglt wherein molecule A has its chain of two peptide units pointing in opposite direction of the chain of molecule B. Pauling and Corey (13) proposed values of $9.46A^{\circ}$ as the translation distance between chains with their amino end and carboxyl end pointing in the same direction. The corresponding distance for Cuglt is $9.316A^{\circ}$. The distance between C_1^{α} and C_3^{α}, which

represents the repeat distance in the pleated sheet configuration was proposed as 6.68A° by Pauling and Corey, and this distance found for molecule A was 6.64A° and for molecule B, 6.59A°. Therefore, the copper chelate of glycyl-l-leucyl-l-tyrosine is in the anti-parallel chain pleated sheet configuration. The values for the anti-parallel pleated sheet configuration as proposed by Pauling and Corey (13) and those found for molecules A and B are summarized in Table 11. A schematic drawing of the anti-parallel pleated sheet configuration is shown in Figure 9.

TABLE 11

Dimensions of Anti-Parallel Pleated Sheet Configuration

	Mol.A	Mol.B	Pauling and Corey Proposed
	129°53'	131°23'	117°48'
	220°22'	218°58'	
a_o	9.316A°		9.46A°
b_o	6.64A°	6.59°	6.68A°

This finding is highly significant in that this is the first observation of a tripeptide or a chelate of a tripeptide existing in the anti-parallel pleated sheet configuration. Furthermore, it is very tempting to suggest that the configuration of the free tripeptide itself exists in the anti-parallel pleated sheet configuration which was

Figure 9. Anti-Parallel Pleated Sheet Configuration (13). Metal M inserted as illustration.

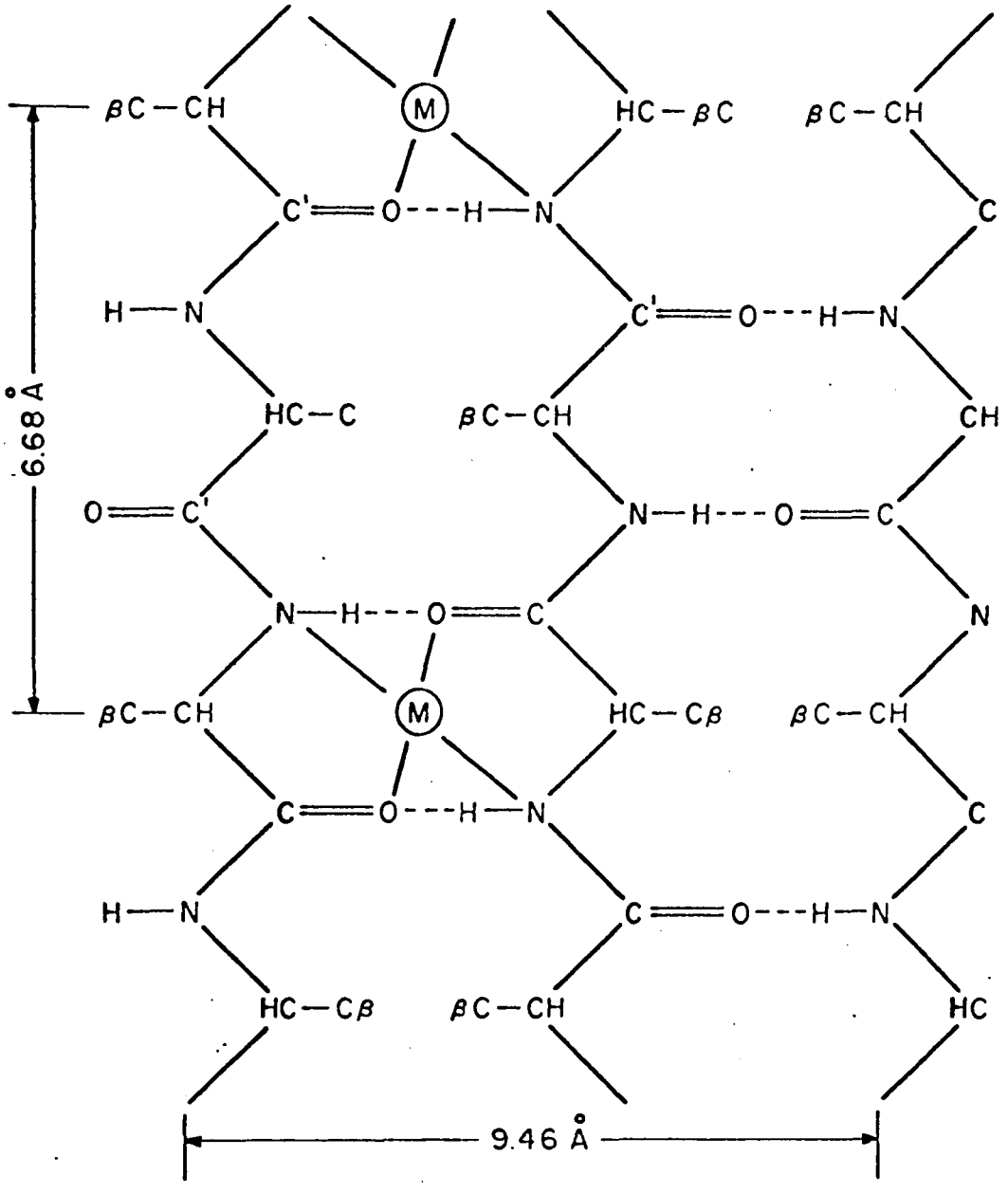

not destroyed upon chelation. The crystal properties of glycyl-l-leucyl-l-tyrosine have been determined by Prof. D. van der Helm as monoclinic, space group $P2_1$, with a β angle of 94.85°, and cell dimensions a_o = 9.36A°, b_o = 21.43A° and c_o = 12.16A°. There were two peptide molecules in the asymmetric unit. The density of the crystals was 1.212 (25°c). The value of a_o of 9.36A° compares favorably with the value of 9.316A° found in the copper chelate and 9.46A° as proposed by Pauling and Corey (13). We can postulate with a reasonable degree of certainty that the free peptide itself does indeed exist in the anti-parallel pleated sheet arrangement. The importance of this finding in small molecules such as glt suggests that any molecules, proteins, polypeptides, tripeptides, etc., that exist in the anti-parallel pleated sheet arrangement can coordinate with a metal ion and still maintain this relative stable configuration. One reason for this could be due to the fact that the configuration of the anti-parallel pleated sheet confers upon the available ligand atoms the same geometry as required by the coordination sphere of the copper ions. This is seen in Figure 9 wherein the metal ion has been placed in the appropriate position between anti-parallel chains. This implies that the peptide molecules themselves exist as a dimer in solution with some type of short range order. It is conceivable that another metal whose coordination geometry is not compatible with

the geometry imposed on the ligand atoms by the anti-parallel pleated sheet configuration would never crystallize because the stable configuration would be destroyed. This would hold especially for larger molecules such as proteins wherein the polypeptide chains cannot orient themselves randomly as can a smaller molecule with a minimum of free energy.

CHAPTER IV

SUMMARY AND CONCLUSIONS

The crystal and molecular structures of the copper chelates of l-serine and glycyl-l-leucyl-l-tyrosine were determined by means of x-ray diffraction. The structure of the copper chelate of l-serine was found to be a dimer consisting of two l-serine molecules and one copper ion. The copper ion of l-serine was five surrounded with the four closest ligands, an amino nitrogen and one carboxylic oxygen from each l-serine molecule, making a distorted square planar arrangement. The fifth position around the copper ion was filled by a carboxylic oxygen, and the sixth position was unoccupied leading to a vacancy in the structure at this location. The hydroxyl group of both l-serine molecules were similar in that they occupied the left-skew position being close to both the amino nitrogen and carboxylic group. The largest difference found between the chelated and unchelated serine molecules was the rotation of the amino nitrogen out of the plane of the carboxyl group in the chelated molecule. The bond distances and angles were normal with one exception which occurred for the angle C_3, C_2, N.

This angle was approximately 4^{o} larger than a normal tetrahedral angle of 109^{o} in both l-serine molecules.

The copper chelate of glycyl-l-leucyl-l-tyrosine was found to contain two copper ions, two peptide molecules, eight water molecules, and one molecule of ether. The chelate was a dimer involving two copper ions, two peptide molecules and a water molecule. Both copper ions were similarly surrounded. The four closest atoms were the amino nitrogen and carbonyl oxygen from the glycyl residues and the peptide nitrogen and a carboxylic oxygen from the tyrosine residues. The fifth position of one copper atom was occupied by a water molecule and the fifth position of the second copper atom was occupied by a carboxylic oxygen from a symmetrically related molecule. The sixth position around both copper ions was vacant. However, the phenolic groups of both molecules were within distances of less than $3.30A^{o}$ from the copper ions at the sixth position.

The ether molecule was used primarily to fill the hole created when the groups of similar polarity located themselves in the same general area. The water molecules were used to fill the cavity between dimers and also to pack dimers by means of hydrogen bonds. Packing within the crystal was further aided by formation of three hydrogen bonds between peptide molecules.

Bond distances and angles were normal within the peptide backbone and compared well with similar results of

other copper chelates of peptides. The more interesting feature of the structure was the orientation of the peptide units. The arrangement of the peptide molecules was the anti-parallel pleated sheet configuration proposed by Pauling and Corey (13). The rotational angles between the peptide units were on the extreme outer limits of the allowed regions computed by Ramachandran and Ramakrismann (15).

In conclusion we can state that the interaction of copper ions with l-serine and glycyl-l-leucyl-l-tyrosine produces no large changes within the molecules themselves when compared with the l-serine itself and available data on unchelated tripeptides and also the models proposed by Pauling and Corey (13).

REFERENCES

1. Shoemaker, D. P., Barieau, R. E., Donohue, J., Lu, Chia-Si, Acta Cryst., 6, 241(1953).

2. Freeman, H. C., Biochemistry of Copper, Peisach, J., Aisen, P., Blumberg, W. E., eds., (Academic Press, New York, 1966), p. 77.

3. Freeman, H. C., Snow, M. R., Tomita, K., Acta Cryst., 17, 1463(1964).

4. Tomita, K., Nitta, I., Bull. Chem. Soc. Japan, 34, 286 (1961).

5. Stosick, A., J. Am. Chem. Soc., 67, 362 (1945).

6. Barclay, G. A., Stephens, F. S., J. Chem. Soc., 2027 (1963).

7. Mathieson, A., Welsh, H. K., Acta Cryst., 5, 599 (1966).

8. Gramaccioli, C. M., Marsh, R. E., Acta Cryst., 21, 594 (1966).

9. Li, N. C., Doody, E., J. Amer. Chem. Soc., 76, 221 (1953).

10. Freeman, H. C., Robinson, G., Schoone, J. C., Acta Cryst., 17, 714 (1964).

11. Freeman, H. C., Schoone, J. C., Sime, J. C., Acta Cryst., 18, 381 (1965).

12. Freeman, H. C., Taylor, M. R., Acta Cryst., 18, 939 (1965).

13. (a) Pauling, L., Corey, R., Proc. Natl. Acad. Sci., 37, 205 (1951). (b) Ibid., 235 (1951). (c) Ibid., 241 (1951). (d) Ibid., 282 (1951).

14. Marsh, R. W., Glusker, J. P., Acta Cryst. 14, 1110 (1961).

15. Ramakrishman, C., Ramachandran, G. N., Biophysical Journal, 5, 909 (1965).

16. T. C. Furnas, Jr., Single Crystal Orienter Instruction Manual, (General Electric, Milwaukee, Wis., 1956), p. 123.

17. H. Lipson, W. Cochran, The Determination of Crystal Structures, Vol. III, (G. Bell and Sons, London, 1953), p. 150.

18. Patterson, A. L., Acta Cryst., 16, 1255 (1963).

19. Beevers, C. A., Robertson, J. H., Acta Cryst., 3, 164 (1950).

20. Wei, L., Stogsdill, R. M., Lingafelter, E. C., Acta Cryst., 17, 1058 (1964).

21. Edsall, J. T., Flory, P. J., Kendrew, J. C., Liquori, A. M., Nemethy, G., Ramachandran, G. N., Scheraga, H. A., Biopolymers, 4, 121 (1966).

22. Ramachandran, G. N., Lakshminarayan, A. V., Biopolymers, 4, 495 (1966).

APPENDIX I

AMPLITUDES AND PHASE ANGLES

TABLE 1

Amplitudes(X10)and Phase Angles of bis(l-Serinato) Cu(II).

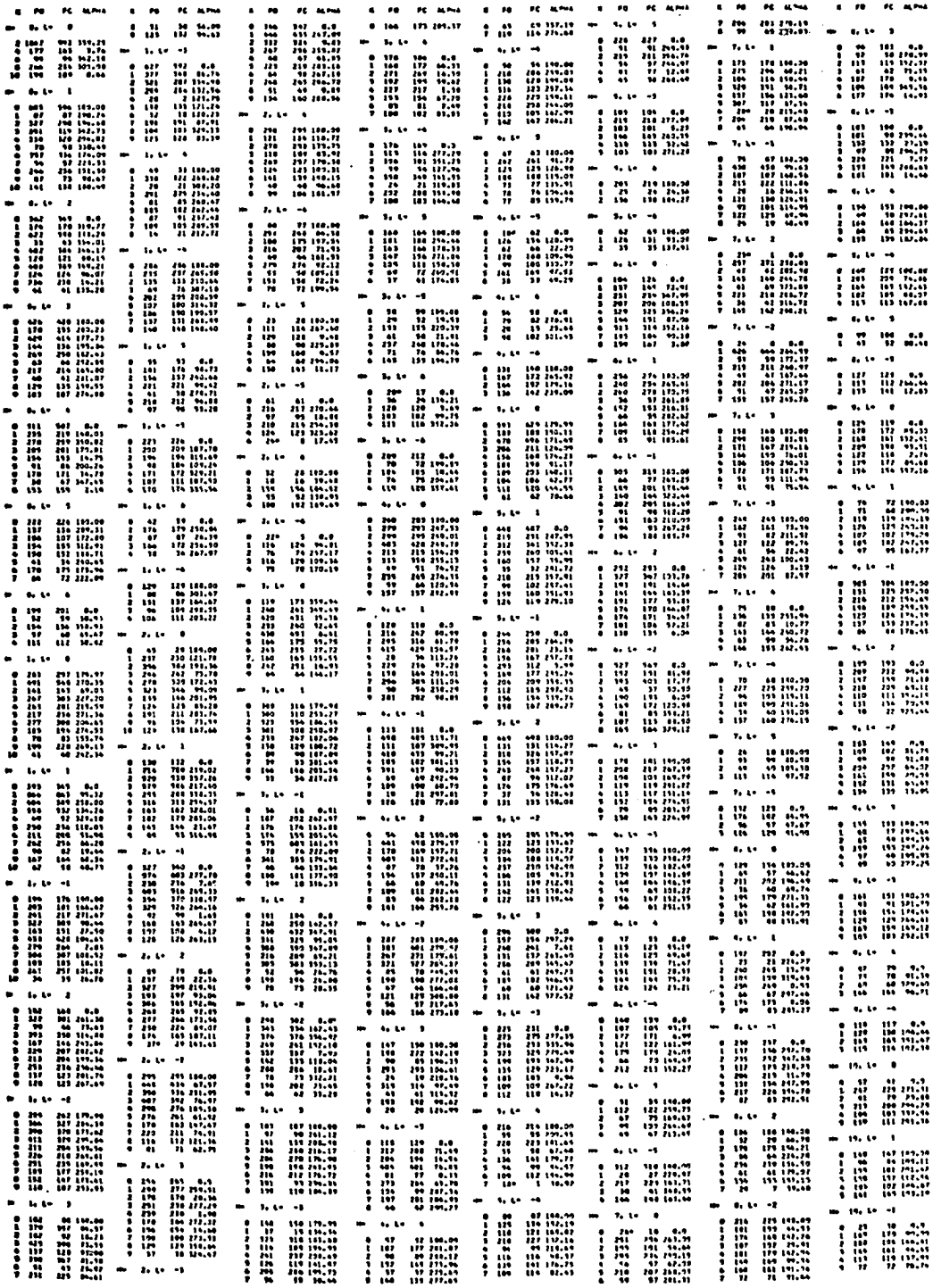

TABLE 1--Continued

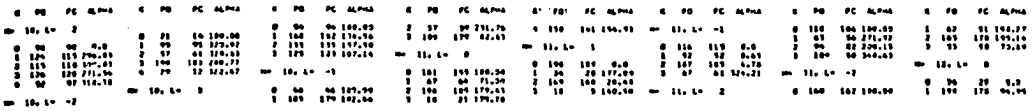

*Unobserved reflections.

TABLE 2

Amplitudes (X10)* and Phase Angles of Cu_2(gly-l-leu-l-tyr)$_2$·$8H_2O$·Et_2O.

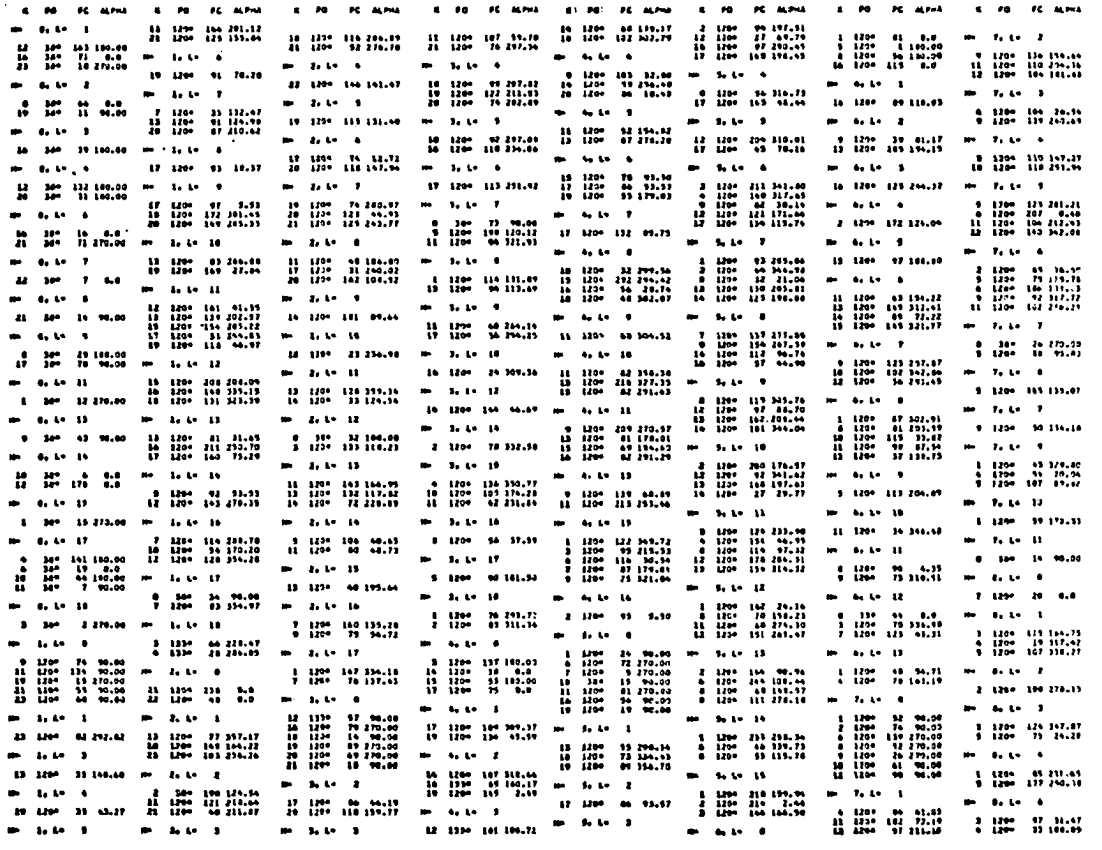

*Unobserved amplitudes.

APPENDIX II

LIST OF COMPUTER PROGRAMS

LIST OF COMPUTER PROGRAMS